MICROPATTERNING NEURONAL NETWORKS ON NANOFIBER PLATFORMS

DISSERTATION

Presented in Partial Fulfillment of the Requirements for the Degree Doctor of Philosophy in the Graduate School of The Ohio State University

By

Veysi Malkoc

Graduate Program in Biomedical Engineering

The Ohio State University

2013

Dissertation Committee:

Professor Derek J. Hansford, Advisor

Professor Yi Zhao

Professor John J. Lannutti

Copyright by

Veysi Malkoc

2013

Abstract

Neuronal networks are groups of interconnected cells in the Central Nervous System (CNS) or the Peripheral Nervous System (PNS) that function in many different ways. They can provide function in the sympathetic nervous system, in a sensory circuit in the spinal column, or can be a high level processing unit in a cortex. If neuronal networks lose their ability to perform their function, this can ultimately lead to a neurological disorder in the body. Therefore it is important to conduct research on neuronal networks to better understand the underlying mechanisms of neurological disorders.

Even though there has been a considerable amount of useful research conducted on neuronal networks, the connections in those neuronal networks are random. There are massive amounts of connections in a mammalian brain, so the ability to guide the connections for studying neural networks is of vital importance. In order to better understand how the brain stores and processes information, the complexity associated with neuronal networks has to be reduced. Cell patterning is a potential solution to this problem and allows simplified and organized neuronal networks.

In this thesis cell patterning using microfabrication techniques is discussed and a microfabricated device that was patterned on biocompatible extracellular matrix (ECM)-

like polymer electrospun nanofibers is introduced. Our device was able to pattern, organize, and simplify neuronal networks. We hypothesized that physical confinement of neural cells and limited routes of neurite extension would contribute to reduced proliferation, increased differentiation, and therefore enable the formation of more robust neural networks. The effect of cell confinement as well as the use of vacuum seeding on neural network formation was compared to cell growth on collagen-coated tissue culture polystyrene and nanofiber mats with no confining microstructures. To test the effects of the underlying nanofibers on the neural network formation, we fabricated our device on both random and aligned nanofibers. We evaluated performance of our device from a neural tissue engineering perspective. Finally, the results of various biological responses, i.e. adhesion, viability, and differentiation, of cells on our devices on random and aligned nanofibers are discussed.

Dedication

This document is dedicated to my wife and to my parents.

Acknowledgments

I'd like to thank my advisor Prof. Derek J. Hansford for his support and giving me the opportunity to work in his research group during my Ph.D. I'd like to thank Prof. John J. Lannutti for his valuable collaboration and guidance. I'd like to thank Prof. Yi Zhao for his great support and guidance.

I'd like to thank biomedical engineering chair Prof. Richard Hart and his staff Melanie Senitko and Kirsten Gibbons for their support and assistance during my graduate work.

I'd like to thank Nanotech West staff Derek Ditmer and Paul Steffen for their technical assistance and support. I'd like to thank Dr. John Merrill for his great support during my graduate teaching assistantship. I'd like to thank all members of Prof. Hansford's group, especially to Dr. Daniel Gallego-Perez, Natalia Higuita-Castro, Dr. Nicholas Ferrell, Dr.Hassan Borteh, and Zachary Rudd.

This research was supported by NSF Nanoscale Science and Engineering Center and Engineering Education Innovation Center at The Ohio State University.

Vita

2000 ..... B.S. Electrical Engineering, Yildiz Technical University, Turkey

2004 ..... M.S. Computer Science, California State University, San Bernardino

2007 ..... M.S. Electrical Engineering, The Ohio State University

2007- 2009 ..... GRA, The Ohio State University

2009- Present..... GTA, The Ohio State University

Fields of Study

Major Field: Biomedical Engineering

Table of Contents

Abstract ii

Dedication iv

Acknowledgments v

Vita vi

List of Tables xxii

List of Figures xiii

CHAPTER 1: INTRODUCTION 1

1.1 Introduction 1

1.2 Microfabrication Techniques 5

1.2.1 Phootolithography 5

1.2.2 Soft Lihography Microtransfer Molding 9

1.2.3 Microcontact Printing 10

1.2.4 Microfluidic Patterning 12

1.3 Cell Patterning 13

1.3.1 Chemical Patterning 13

1.3.2 Physical Patterning 18

1.4 Electrospun Polymer Nanofibers 20
1.4.1 Electrospinning Process 21
1.4.2 Electrospinning Parameters 22
1.4.2.1 Electric Field Strength 22
1.4.2.2 Flow Rate 23
1.4.2.3 Collector Distance 23
1.4.2.4 Solution Concentration 23
1.4.2.5 Solvent Volatility 24
1.4.2.6 Solution Conductivity 24
1.4.3 Tissue Engineering 25
1.4.3.1 Material Choice 25
1.4.3.2 Fiber Orientation 26
1.4.3.3 Porosity/Pore Size 27
1.4.3.4 Surface Modification 28
1.4.3.5 Controlling Nanofiber Morphology 28
1.4.3.6 Bone Tissue Engineering 29
1.4.3.7 Tendon/Ligament Tissue 29
1.5 Neural Tissue Engineering 30
1.5.1 Differentiation of Neural Stem Cells 31
1.5.2 Neurite Outgrowth 32
1.5.3 Repairing Peripheral Nerve Defects 34
1.6 Conclusions 35

CHAPTER 2: CONFINED NEURONAL NETWORK DESING AND FABRICATION 36
2.1Introduction 36
2.2 Materials and Methods 36
2.2.1 Device Geometry 36
2.2.2 Silicon Wafer Patterning 37
2.2.3 PDMS Molding 39
2.2.4 Electrospinning Gel/PCL Nanofibers 39
2.2.5 Microtransfer Molding 40
2.2.6 Double Stamp Micromolding Technique 41
2.2.7 Stamping of the CNN 42
2.3 Results and Discussions 43
2.4 Conclusions 44
CHAPTER 3: MICROPATTERNING NEURONAL NETWORKS ON NANOFIBER PLATFORMS 45
3.1 Introduction 45
3.2 Materials and Methods 47
3.2.1 Materials 47
3.2.2 Device Fabrication 47
3.2.3 Fabrication of Electrospun Random Nanofibers 49

3.2.4 Collagen Coating onto Electrospun Random Nanofibers 50
3.2.5 Characterization of the Electrospun Nanofibers and the Fabricated Microdevice 50
3.2.6 Vacuum Assisted Cell Seeding 50
3.2.7 Sample Types 51
3.2.8 In Vitro Cell Culture 51
3.2.9 Cell Adhesion Assay 52
3.2.10 Cell Viability Assay 52
3.2.11 Immunocytochemistry and Neurite Length 52
3.2.12 Statistics 54
3.3 Results and Discussions 54
3.4 Conclusions 63
CHAPTER 4: EFFECTS OF CELL CONFINEMENT AND NANOFIBER ORIENTATION ON NEURONAL NETWORK DIFFERENTIATION 64
4.1 Introduction 64
4.2 Materials and Methods 65
4.2.1 Materials 65
4.2.2 Device Fabrication 66
4.2.3 Fabrication of Electrospun Aligned and Random Nanofibers 67
4.2.4 Collagen Coating onto Electrospun Aligned and Random Nanofibers 68

4.2.5 Characterization of the Electrospun Aligned and Random Nanofibers and the Fabricated Microdevice 68
4.2.6 Vacuum Assisted Cell Seeding 69
4.2.7 Sample Types 69
4.2.8 In Vitro Cell Culture 70
4.2.9 Cell Viability Assay 70
4.2.10 Immunocytochemistry and Neurite Length 71
4.2.11 Statistics 72
4.3 Results and Discussions 72
4.4 Conclusions 80
CHAPTER 5: CONCLUSIONS AND FUTURE WORK 81
LIST OF REFERENCES 84

List of Tables

Table 1. Neurological disorders and the number of people affected in the world 2

List of Figures

Figure 1.1 Photolithography Steps 8

Figure 1.2 Molding PDMS Negative Replica and Microcontact Printing 11

Figure 1.3 Signaling pathways for PC12 cell differentiation and neurite extension, modified from [114] 34

Figure 2.1 Confined Neuronal Network (CNN) 37

Figure 2.2 (A) Patterned Silicon Wafer (B) SEM image of the PDMS Mold 38

Figure 2.3 Fabrication steps of the CNN device 43

Figure 3.1 Fabrication of the CNN Microdevice 48

Figure 3.2 (A) PDMS Mold (B)Polymer Dewetting (C) Polymer removed from raised features (D) PS features standing on peeled off PVA film (E - F) Fabricated CNN Microdevice 55

Figure 3.3 (A - B) Electrospun Random Gel/PCL Nanofibers 56

Figure 3.4 Cell Patterning on CNN Microdevice (green alexa fluor 488 phalloidin) 56

Figure 3.5 Representative images for attachment of PC12 Cells on: (A) nonvacuum; (B) collagen_fiber; (C) noncollagen; (D) device. (E) Cell Attachment (% TCPS) 57

Figure 3.6 Viability of PC12 Cells on nonvacuum, collagen_fiber, noncollagen, device 58

Figure 3.7 Representative images for viability of PC12 cells on: (A) nonvacuum; (B) collagen_fiber; (C) noncollagen; (D) device. (left, 1 day; right 3 days; green alexa fluor 488 phalloidin) 59

Figure 3.8 Differentiation of PC12 cells on: (A) nonvacuum (B) collagen_fiber
(C) noncollagen (D) device 61

Figure 3.9 (A) Differentiation Ratio and (B) Neurite Length (μm) 61

Figure 4.1 Fabrication of the CNN Microdevice on Electrospun Aligned nanofibers 67

Figure 4.2 (A) PDMS Mold (B)Polymer Dewetting (C) Polymer removed
from raised features (D) PS features standing on peeled off PVA film
(E - F) Fabricated Microdevice on Aligned Nanofibers 73

Figure 4.3 (A - B) Electrospun Random Gel/PCL Nanofibers
(C - D) Electrospun Aligned Gel/PCL Nanofibers 74

Figure 4.4 Viability of PC12 Cells on long, short, aligned and random 75

Figure 4.5 Representative images for viability of PC12 cells on:
(A) long; (B) short; (C) aligned; (D) random. (left, 1 day; right 3 days;
green alexa fluor 488 phalloidin) 76

Figure 4.6 Representative images for Differentiation of PC12 cells on:
(A) long; (B) short; (C) aligned; (D) random. (left, 2 days; right 4 days;
green alexa fluor 488 phalloidin) 77

Figure 4.7 Differentiation Ratio 78

Figure 4.8 Average Neurite Length per Differentiated Cell (μm) 78

CHAPTER 1: INTRODUCTION

1.1 Introduction

Neuronal networks are groups of interconnected cells that can be a tissue slice, a population of cells *in vivo*, or a cultured group of cells *in vitro*. Neuronal networks are found in the Central Nervous System (CNS) or the Peripheral Nervous System (PNS) and can function in many different ways. They can be functioning unit in the sympathetic nervous system, a sensory circuit in spinal column, or a high level processing unit in a cerebral cortex. If neuronal networks lose their ability to perform their function, it ultimately leads to a neurological disorder in the body. In order to better diagnose and develop therapeutics for neurological disorders, it is important to better understand the underlying mechanisms of neurological disorders, and thus conducting research on neuronal networks becomes crucial for seeking cures for neurological disorders.

The World Health Organization (WHO) presented a report on the global burden of neurological disorders in 2005, which reported that approximately 1 billion people in the world are affected by neurological disorders. Table 1 shows the number of people affected by various neurological disorders [1]. Taking these large number of patients into account, there is a strong motivation to study neuronal networks and explore therapeutics for neurological disorders.

Epilepsy is a neurological disorder that causes people to have recurring seizures. The seizures are due to anomolous signals that originate from a misfiring group of cells (the epileptic focus) in the patient's brain. Seizures can cause violent muscle spasms, and in extreme cases can cause the patient to lose his/her consciousness.

	Millions of patients
Epilepsy	39.8
Alzheimer's disease	24.4
Parkinson's disease	5.2
Multiple sclerosis	2.4
Migraine	326.1
Cerebrovascular disease	61.5
Neuroinfections	18.1
Nutritional neuropathies	352.4
Neurological injuries	170.3

Table 1. Neurological disorders and the number of people affected in the world [1]

An example of clinical research on epilepsy mitigation was presented by Yamamoto, *et al*. [2], who conducted a study on a 31 year old male patient with intractable epilepsy. The term intractable epilepsy refers to the fact that the patient did not respond to medication. The patient had seizures on average 1 to 3 times per month. A magnetic resonance imaging (MRI) of his head showed a left hippocampal atrophy and a streak cavity in the left mid-to-posterior temporal region. Three subdural grid electrodes

manufactured by Ad-Tech Co. with 1 mm diameter electrodes were implanted into the patient's left temporal lobe. Interictal discharges were mostly seen at electrodes A1 and A9, so these regions were targeted for cortical electrical stimulation. Initially, 7.5 mA and then 2mA with 0.9 Hz pulses were tried. However, these resulted in aura (smaller scale seizure), so stimulation was reduced to 0.5 mA pulses. After the second stimulation session, the epileptiform discharges were reduced, and were minimal after the third stimulation session. After determining the seizure onset-zone, the patient had left temporal lobectomy and had no seizures 10 months after surgery. The results demonstrated that depending on the stimulation intensity, both excitatory and inhibitory effects could be seen. Inhibitory effect was seen with 0.5 mA pulses and was chosen as the stimulation protocol to be applied to the patient since stimulations greater than this intensity caused excitatory effects leading to epileptiform discharges.

There has been interest on conducting research on neuronal networks *in vitro* as well. Microelectrode arrays offer the opportunity of both stimulating and recording from a culture at the same time. As the number of microelectrodes increases, the information extracted from the neuronal network becomes more detailed. Cultured neuronal networks output spontaneous bursting activity. Learning a new task requires an association between the stimulation and its response. Following this association, neuronal networks are then able to modulate their firing activity. Li, *et al*.[3], investigated and modeled learning in a cultured neuronal network by applying low frequency stimulations (0.2 Hz). Hippocampal neurons were cultured on microelectrode arrays and allowed to mature. They used a training protocol in which a series of 300 stimulations were applied through

a pair of electrodes and the responses were recorded from the remaining electrodes. 10 minutes was given for a stimulation trial to elicit a response from the network. If there was no response, or the desired stimulus to response ratio (2/10) was not achieved, then this was called a "non-learning" state. They also had controls that did not undergo any training session. Spontaneous activities of controls, non-learning, and learning states were compared. There was no significant difference between the non-learning and control states, which were randomly firing, while the learning neuronal networks developed an organized and increased bursting activity. The number of bursts was increased 154% after learning. They demonstrated that a cultured neuronal network can learn with a training protocol and be modulated according to desired outputs.

Even though there has been a considerable and useful amount of research conducted on neuronal networks, the connections formed in these neuronal networks are random, and still fall well short of the massive amounts of connections to properly model an *in vivo* neural network. A mammalian CNS, specifically the brain, is highly complex and there are 80-120 billions of neurons, each with thousands of connections. In order to better understand how the brain stores and processes information, the complexity associated with neuronal networks has to be reduced. Cell patterning is a potential solution to this problem and allows simplified and organized neuronal networks.

Microfabrication is the term that describes the steps needed to fabricate miniaturized structures. Several microfabrication techniques exist and are used for cell patterning. Those techniques allow us to understand fundamental studies in cell biology such as cell-substrate, cell-cell interactions [4].

1.2: Microfabrication Techniques

Microfabrication techniques are photolithographic patterning, soft lithography microtransfer molding, microcontact printing and microfluidic patterning.

1.2.1 Photolithography

Photolithography is the term used to describe the transfer of a pattern from a photomask onto a substrate by selectively exposing the coated photosensitive polymer (photoresist) using ultraviolet (UV) light (Figure 1.1).

The basic steps for photolithography are: substrate preparation, photoresist coating, pre-bake, exposure, post-exposure bake, developing, rinsing and drying. Substrate preparation involves cleaning and priming. The substrate can be a silicon wafer or a glass wafer. Cleaning is done with dipping the substrate into a piranha tank at 120 ^{o}C. Piranha solution is prepared by mixing 3:1 sulfuric acid (H_2SO_4) and hydrogen peroxide (H_2O_2). Priming involves increasing adhesion between the substrate and the photo resist. Photo resists especially positive one do not adhere well to the substrate. This effect is more pronounced when there is high humidity in the environment. For this purpose, an adhesion promoter called hexamethyldisilazane (HMDS) is widely used in vapor phase. Treatment occurs temperatures above 150 ^{o}C in an oven so that any adsorbed water can be driven away. This promoter then makes strong chemical bond (silylation) with the oxide surface. Applied photoresist is then able to adhere to methyl groups of HMDS.

Photoresist coating is done by spinning the photoresist onto the substrate. The photoresist is dispensed onto the wafer which sits on a platen in a resist spinner. Applied vacuum holds the wafer in place. The wafer is spun at high speeds between 1500 and 6000 rotations per minute (RPM). The uniform film thickness depends on the spin speed, concentration and the viscosity of the solution. After spin coating the photoresist, it can still hold up to 15% solvent and embedded stresses. A soft bake (pre-bake) step, up to 10 min depending on the thickness, at 65-115 ^{o}C then drives away the remaining solvent and stresses.

After the soft bake, the wafers are exposed to UV light by aligning them to the photomask. This exposure and alignment can happen multiple times if there are multiple layers of photoresist to be exposed. The wavelengths of the light source used range from extreme UV 10-14 nm to deep UV 150-300nm and to near UV 350-500 nm. In near UV , commonly a mercury lamp is used as the source and its wavelengths are i-line (365 nm) and g-line (435 nm). When the incident light intensity (W/cm^2) is multiplied by the exposure time in seconds, it gives the incident energy (J/cm^2) across the photoresist film. Exposure of light induces a chemical reaction in the exposed areas where the solubility in a developer changes between the exposed and unexposed regions in the photoresist. Post exposure bake is required when the chemical reaction in the exposed areas is not complete and need temperature to catalyze the reaction.

The tone of the photoresist determines solubility in the development after the exposure. Photoresists have 3 basic components: a base resin, a photo active compound and a solvent. If the photoresist is positive (AZ5214), the photo chemical reaction during

exposure weakens the bonds between resin in the exposed areas and it becomes more soluble in the developer. If the photoresist is negative (SU8), then the exposed regions cross-link and solubility is highly reduced compared to unexposed areas.

Development is the step to dissolve and remove undesired regions of the photoresist. If the photoresist is negative, usually organic solvents are used and if it is positive alkaline based solvent such as KOH are used. Rinsing occurs with deionized water for positive resist and isopropyl alcohol for negative resists followed by blow drying the wafer with nitrogen [5,6].

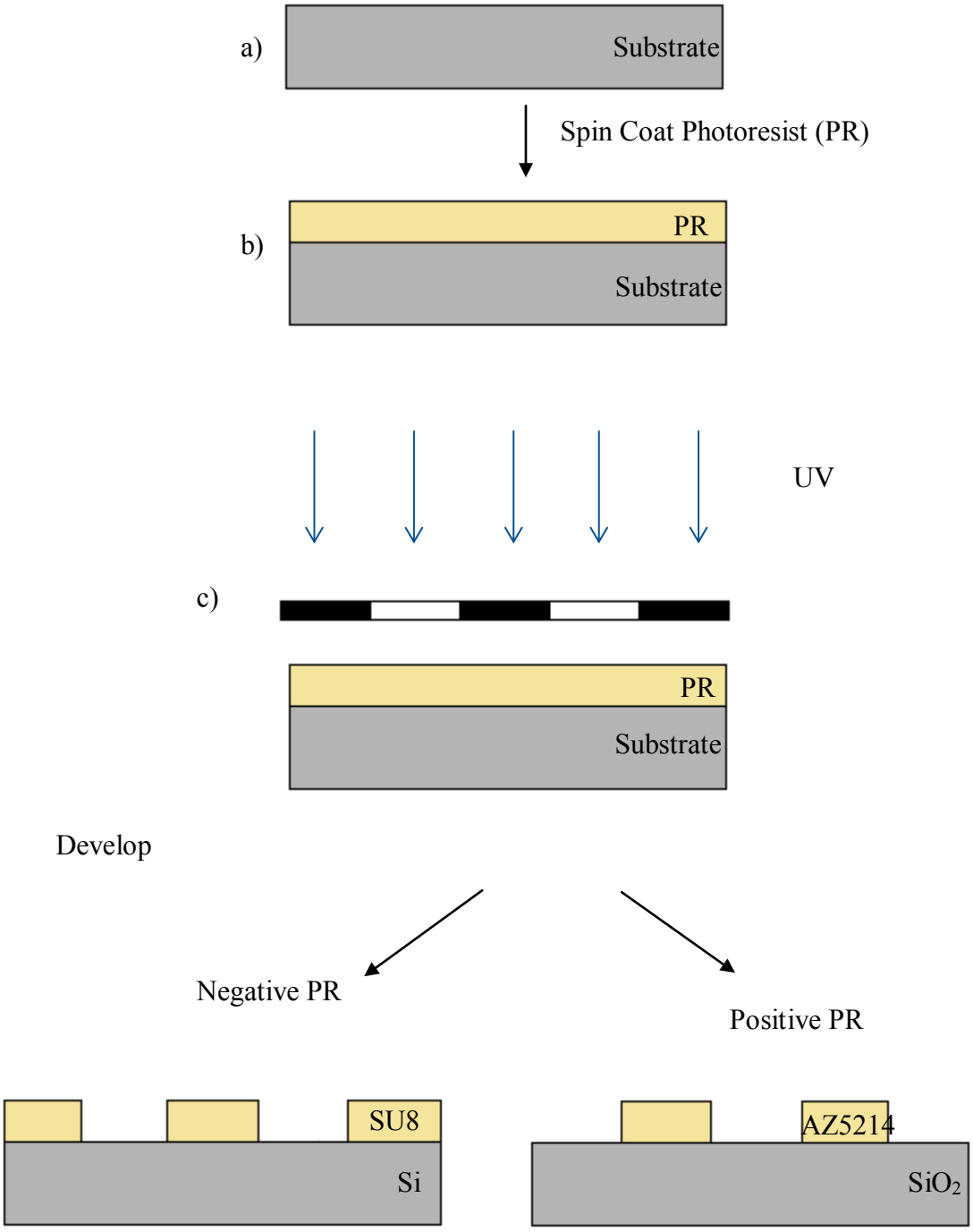

Figure 1.1 Photolithography Steps

1.2.2 Soft Lithography Microtransfer Molding

Soft lithography is a set of techniques used in micro/nano fabrication and is based on printing and molding patterns using an elastomeric mold. Soft lithography has many advantages over photolithography. In particular, we are able to modify molecular structure of surfaces and pattern biomolecules and can pattern cells with microfluidic compartments. This is a relatively inexpensive and convenient technique used in microfabrication. [7].

Self assembled monolayers (SAMs) allow molecular level surface modification. Soft lithography techniques utilizing SAMs enhance surface modification and patterning capabilities dramatically. A very common use of SAMs is alkanethiolates on gold. Gold reacts with thiol groups and forms SAMs. The end group of SAMs is a small, nonpolar, organic functional group and allows us to tailor the surface properties. For example, this end group can be a ligand for an enzyme or a tripeptide that is specific to integrin receptors of mammalian cells. This surface is then now able to bind to proteins or conducive to attachment of mammalian cells [7].

The key step in soft lithography is to replicate the master with an elastomer. Polydimethylsiloxane (PDMS) is widely used as an elastomer to fabricate the negative replica of the master. First, the silicon master is fabricated using photolithography. Next, PDMS prepolymer is mixed with a curing agent and poured onto the silicon master. After waiting at room temperature for 48 hrs, the PDMS polymer is cross linked and is peeled off from the master. The peeled off mold is then a negative replica of the silicon master (Figure 1.2). The Young's modulus of PDMS is 1 MPa and thus is a moderately stiff

elastomer. It is biocompatible and optically transparent. Naturally, PDMS is hydrophobic but can be turned into hydrophilic phase with oxygen plasma treatment.

Microtransfer molding (μTM) includes applying a liquid prepolymer onto a PDMS mold. The excess polymer is removed by blowing nitrogen and the mold is brought into contact with a substrate. The prepolymer is cured with exposing it to either UV or heat. After curing, the PDMS mold is removed and now the pattern which is the raised features on the mold is transferred onto the substrate as a cured polymer. Microtransfer molding will be discussed in more detail in chapter 2 of this theses [8].

1.2.3 Microcontact Printing

Microcontact printing was first developed as an alternative to photolithography by Whitesides and his coworkers in 1993 [9]. They patterned SAMs of alkanethiols on gold substrates. An inking solution is applied to a PDMS mold which has the desired pattern on it. The pattern to be transferred is on the raised features. After a few minutes of applying inking solution, the excess is blown dry with nitrogen. Then the PDMS mold is brought into contact with the substrate for a few seconds and then removed. The PDMS mold ensures conformal contact and the ink is transferred to the substrate from the desired raised features on the mold (Figure 1.2).

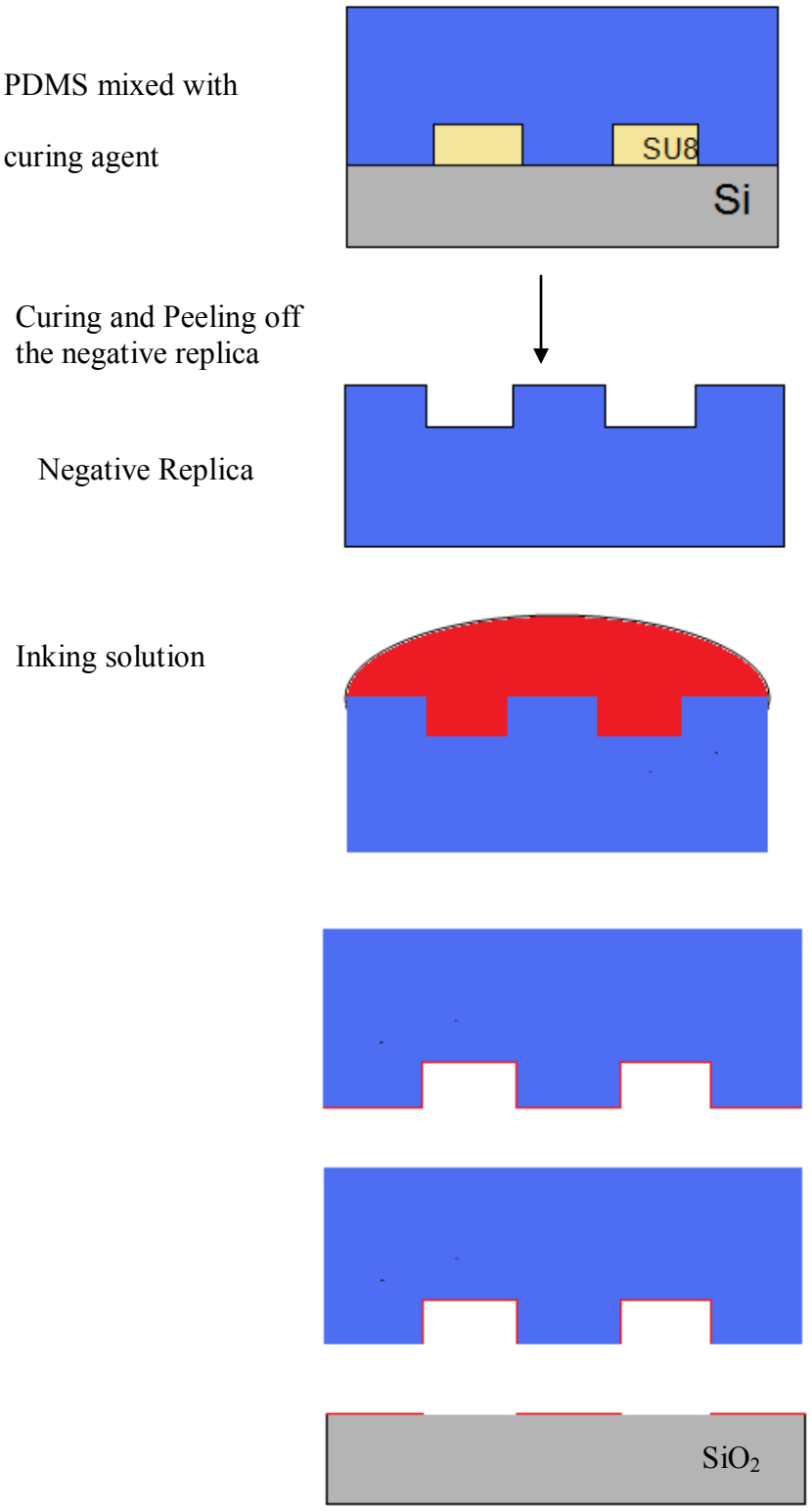

Figure 1.2 Molding PDMS Negative Replica and Microcontact Printing

Mechanical stability of the PDMS mold allows high pattern resolution and contrast. In addition, the adsorbed protein is stable in terms of its biological activity [10].

1.2.4 Microfluidic Patterning

Microfluidic patterning is to pattern a substrate by running a solution inside the micro channels. The micro channels in PDMS are sealed onto the substrate and fluid flows only inside those microfluidic channels. The sealed portions of PDMS are protected from any sort of modification and thus allow a pattern on the substrate to be generated. Untreated PDMS surface will hinder flow and therefore one requirement for microfluidic channels in PDMS is to treat the channels with oxygen plasma so that they turn into hydrophilic state and facilitate the flow.

The flow regime in microfludic channels for patterning the substrate for biological applications is laminar. Laminar flow is a type of flow with low Reynolds number where two streams flow side by side and do not disturb each other. Diffusion takes place only at the interface of two streams. Reynolds number is a dimensionless number which gives the ratio of inertial forces to viscous forces. Microfluidics where channel width is ~100 μm for biological applications runs with low Reynolds number of ~1 [7, 11, 12].

Taylor et al. have patterned microfluidic channels of 25 μm wide with 25 μm spacing. The channel depth was 50 μm.The mold was a PDMS negative replica of a silicon wafer which was patterned with SU-8 50 by using photolithography. 50 μg/ml of

poly-L-lysine (PLL) in sterile deionized (DI) water was allowed to fill the microfluidic channels. Incubation time was 1 hour and during this time adsorption of PLL occurred on the substrate where the microfluidic channels were running. The left side of the channel is somatic side whereas the right side is for neuritic extensions only. The microfludic channel serves as a guide for the neuron to make connections through the other end of the channel. On the somatic side, embryonic rat cortical neurons (E18) were cultured and allowed to make connections along the channel to the neuritic side. This type of patterning can be used for Alzheimer's disease where certain pharmaceuticals can be applied to a neuron's different sections at the same time or only to one portion of it. After 4 days of culturing E18 cortical neurons, the neuritic extensions were seen traveling within the pattern where there is PLL and reaching to the neuritic region. There is no neuritic extension in between PLL coated lines since neurons preferentially attach to PLL regions [13] .

1.3 Cell Patterning

There are two types of cell patterning: chemical and physical (topographical).

1.3.1 Chemical Patterning

The chemistry of the surface of a substrate is well known to affect cellular attachment and spreading. Water contact angle (WCA) measurements are one aspect of identifying surface chemistry such that whether it is hydrophobic or hydrophilic. WCA is a common technique applied and conforms well with the cell response to a surface. The

hydrophocity and hydrophilicity of the surface determines whether a protein adsorbs to a surface, being displaced or encounters any conformational changes. Cell culture medium is supplemented with serum proteins and when cells encounter a surface, they do not see a bare surface instead a surface adsorbed with serum proteins. This adsorbed layer interacts with cell receptors and integrins on cell surface so that ultimately cellular attachment and spreading can occur. Leo Vroman was the one who first described adsorption, displacement and conformational changes of proteins. Most mobile and smaller proteins such as albumin first adsorbs to the surface and is being displaced by larger proteins such as fibronectin which contains cell adhesive peptides in contrast to cell repellant albumin [14, 15, 16]. Hydrophobicity of the surface determines ultimate displacement of the proteins. Albumin on a more hydrophobic surface, exposes its hydrophobic core and shields it from aqueous environment, thereby changing its conformation from a native state to a denatured one. This denatured state increases albumin binding to the surface and decreasing the probability of a larger protein to displace it [17]. Hydrophilic surfaces also have been shown to allow cell attachment, spreading and proliferation. The more hydrophilic the surface, the better the cellular adhesion is [18]. A hydrophilic amine surface is shown to be a favoring environment for fibroblasts adhesion [19].

SAMs allows to study chemical interactions between biological species and a surface. SAMs molecules are closely packed on the surface. The molecular layer binds to the thiols on the surface through thiolate bonds when the surface is gold or silver and siloxane bond when silanes are used on oxides. Terminal groups of SAMs can be

alcohols, alkenes, carboxylic acids and primary amines. Whitesides et al. were the first group who demonstrated use of SAMs to alter the surface hydrophobicity/hydrophilicity and therefore protein adsorption [20]. Sorribas et al. have patterned dorsal root ganglion cell cultures on rectangular grid patterns on glass using photolithography. First, they have immobilized axonin-1 which is a neuronal membrane bound glycoprotein found in developing axonal tracts on glass [21]. Then, it was protected with sucrose for subsequent photolithography processes. After photolithography, oxygen plasma is used to etch the exposed areas, thereby removing sucrose and the protein therein. Immobilization of axonin-1 is obtained by treating the surface with aminopropyltriethoxysilane (APTES) and using N-[γ-maleimidobutyryloxy]sulfosuccinimide ester (sGMBS, Pierce) as a cross linker to cysteine (thiol groups) on the peptide. Immobilization of the protein is confirmed with immunochemistry and neuronal cells were preferentially attached to the line crossings and neurites grew and aligned in the direction of the lines [22]. Laminin is a family of gylcoprotein found in basal lamina. They are important in cellular adhesion, differentiation and migration. They are also important for neuronal outgrowth. Vogt-Eisele et al. have patterned a rectangular grid of a PA-22 which is A chain of laminin to culture rat embryonic cortical neurons. A glass surface is treated with first aminopropyltrimethoxysilane (APTMS) and then with the cross linker sGMBS.

A PDMS mold is fabricated which contains the desired pattern. Inking solution, PA-22 is applied to the mold for 20 minutes and blown dry with nitrogen. Using microcontact printing the mold is contacted to the treated substrate and a pattern of PA-22 is formed on the substrate where mold contacted. Terminal thiol groups on PA-22

covalently binds to the treated glass surface [23, 24]. Cell adhesive protein fibronectin is shown to adsorb onto hydrophilic areas by Mcfarland et al. when the surface was patterned with photolithography and alternating regions of hydrophilic amines adjacent to dimethyldichlorosilane regions were created [25]. Buzanska et al. seeded human umbilical cord blood derived neural stem cells on an array of square patterns in which interconnecting lines provided the communication between squares. Cell adhesive area was coated with fibronectin and allowed spreading and neuronal commitment of neural stem cells [26].

Xing et al. have fabricated laminin stripes on a Poly-L-Lysine (PLL) background. They have used rat hippocampal neurons for this study. Laminin stripes are fabricated through microcontact printing from a PDMS mold that is inked with laminin solution. They have examined the growth cone behavior on laminin patterns with varying concentrations. They have found that growth cone responds to concentration gradient that is steepest between PLL and laminin. The growth cone travels within the boundary of PLL and laminin [27].

To pattern cells, cell adhesive and repellant areas are commonly used. One technique to pattern cell repellant areas is to coat it with polyethylene glycol (PEG). PEG is a hydrophilic polymer and has antifouling properties. It prevents protein adsorption to the surface and thus is a strongly cell repellant polymer [28]. Ruiz et al have patterned PLL squares on a PEG background. PLL squares are created with microcontact printing with a PDMS mold inked with PLL solution. PEG is deposited through plasma polymerization in a capacitvely coupled radio frequency plasma system. 20 nm thick

PEG layer was deposited onto glass surface. They have used human umbilical cord blood neural stem cells in their experiments. Cells were successfully patterned and localized on the squares, the cell pattern was stable up to 4 weeks and after 6 days of seeding, neuronal outgrowth was observed.

Plasma etching is another way of modifying surface properties. If oxygen species are incorporated into plasma, surface wettability is altered leading to a more hydrophilic surface. One of the most common application is to treat polystyrene surface with oxygen plasma and render it more hydrophilic [29]. Bruil et al. showed that polyurethane film was first exposed to tetrafluoromethane plasma and then to argon plasma thus leading to a more hydrophilic surface. Therefore, since surface wettability is increased they have observed more leukocyte adhesion on these areas [30].

PLL coated substrates contain positively charged hydrophilic amine groups, promote cellular adhesion and allow a neuronal network to be formed. Hwang et al. have patterned Fluorescein isothiocyanate (FITC) conjugated PLL patterns on a glass substrate. They have fabricated the PDMS mold from a photomask film which is printed through a conventional laser printer. FITC-PLL patterns sare produced through microcontact printing. The pattern of dots with interconnecting lines was verified with fluorescence microscopy. They have seeded hippocampal neurons from E-18 Sprague-Dawley rat onto the patterns and after 3 days a neuronal network on PLL grid pattern was formed [31].

1.3.2 Physical Patterning

Substrate topography is modifying the surface without any biomolecule and providing an extracellular physical milieu for the cells. *In vivo,* cells do not interact with a smooth surface rather it is a textured surface that they interact with. This textured surface is composed of pit, pores, striations, particulates and fibers. This is the motivation leading to patterning cells on physical patterns. Pyhsical patterning is classified in terms of directionality of the patterning; anisotropic and isotropic. Anisotropic features such as ridges and grooves are patterned to see if they provide alignment of the cells along the direction of the features whereas isotropic features are examined for their effects on collective cell functions. Contact guidance is the phenomenon by which physical patterns on a substrate guide the cellular alignment and elongation. During nervous system development physical structure of the surface strongly influences developmental stages. During development, radial glia are organized into regular arrays that guide migration of embryonic neurons [32].

Cell orientation generally increases with increasing groove depth but decreases when the groove width or pitch increases. If the pitch becomes larger than the cell, cell tends to traverse the pitch rather than aligning with the grooves [33, 34, 35, 36]. Teixeira et al. showed that human corneal epithelial cells align on 70 nm wide grooves that are fabricated through electron beam lithography (EBL) [37]. EBL is a type of lithography that patterns a resist on a surface by scanning it with emitted electron beams and gives nanoscale resolution.When the groove depth is too high and the width is too small, cells

tend to bridge in between ridges [34,35]. Shain et al. have patterned varying sizes of pillars with different spacing to examine topographical effects on hippocampal neuronal growth. The surface is treated with PLL and features were patterned using photolithography. B_{III} – tubulin immunocytochemistry was used to observed neuronal processes and outgrowth. They found that 2 μm wide pillars with 1.5 μm spacing had the best orthogonal alignment of neurites on pillars compared to smooth surfaces and other pillar geometries [38]. Fozdar et al examined the effects of features sizes and shapes on rat embryonic hippocampal cells. The patterns are fabricated using electron beam lithography. They have patterned holes and lines of 2 μm and 300 nm for each feature type. They have placed cells between two different topographies or to a topography with a certain distance. Cells placed at a distance of 30 μm or less were able to choose topography over a smooth surface. 300 nm perpendicular lines and 300 nm holes were favorable for cells to grow axons on. These results corroborate the earlier reported ones that cells interact with a topographical surface *in vivo*. Gomez et al. also found that rat embryonic hippocampal neurons preferred 1 μm over 2 μm lines which may suggest that smaller features mimic *in vivo* characteristics more [39].

Isotropic microtopography often times gives inconsistent results in terms of cellular response. Fibroblasts had a greater proliferation on 2 μm diameter nodes than on 2 μm wells whereas when both features had a diameter of 10 μm , there was not a significant difference [40]. Cell response on isotropic features can degrade compared to smooth(non-processed) surfaces. Macrophage spreading was much less on 5 μm pillars than a smooth surface [41].

In addition to patterning cells either chemically or physically, it is also possible to combine and use both techniques at the same time. Zhang et al. have first patterned negative resist of SU8 nodes with interconnecting lines using photolithography. Second, with a reverse mask and carefully aligning a positive photoresist is patterned on top of it so that it can serve as a lift-off layer for PLL deposition. Embryonic rat hippocampal neurons are seeded for their study and a neuronal network and neurite elongations were seen within the barriers of negative resist. Electrophysiological recordings proved that there is functioning electrical activity and neurons are healty [42]. Miller et al. have also examined synergistic effects of chemical and physical guidance on neurite alignment and outgrowth. A blend of poly-D-L-lactic acid (PDLA) and poly (lactide-co-glycolide) PLGA 85:15 film was produced using solvent-cast technique. The master pattern on silicon and quartz were fabricated using photolithography and ion etching. Patterns were transferred to the polymer film with compression molding. Laminin was absorbed into the grooves through surface tension. Groove depths greater than 2 μm had a better alignment of neurons. Laminin coated films had better adhesion and neurite alignment. Grooves with 4 μm deep and no laminin coated had 86% alignment whereas when laminin coated it increased to 92% alignment [43].

1.4 Electrospun Polymer Nanofibers

Recently there has been great interest in electrospun polymer nanofibers. Electrospun nanofibers provide the fiber diameters to be at nanoscale and its fibrous morphology mimicking extracellular matrix (ECM) is a great advantage for tissue

engineering applications and to study cellular microenvironment. Electospun nanofibers have high porosity and large surface area. They can be functionalized with native ECM proteins and enhance cellular attachment, differentiation, proliferation and migration. Electrospun nanofibers can be aligned in unidirectionally and enhance neuronal outgrowth. A fiber mat in the form of 2D or 3D scaffold can be obtained for tissue engineering applications.

1.4.1 Electrospinning Process

An electrospinning setup includes a metal capillary, a high voltage source and grounded collector. Capillary is attached to a syringe which contains the polymer solution. A syringe pump is used to push solution inside the syringe and obtain the desired flow rate. High voltage source is applied to this metal capillary and circuit is completed with the grounded collector .

Applied high voltage induces free charges in the polymer solution and these charges move to the opposite polarity of collector because of the applied external electric field. At the tip of capillary, the pendant drop of solution turns into a cone like shape due to the tensile forces applied on it. Taylor showed that there is an equilibrium between the surface tension of the pendant drop and applied voltage when there is 49.3^{o} angle on the cone. Hence, this is called Taylor cone. When the surface tension of the pendant drop can no longer compete with the applied external voltage, a jet is imitated at the tip of the cone. This jet continuously thins down along its travel to the grounded collector and being accelerated in the direction of applied electric field due to the charged ions in the

polymer solution. The jet experiences a chaotic motion or bending (whipping) instability due to the repulsive forces between charged ions in the solution and produces a electrospun nanofibers mat on the grounded collector. Originally, this instability was thought to be happening due to "splaying" of the jet into multiple smaller diameter jets. However, recently Warner et al. and Shin et al. have used high speed of photography which can take pictures down to 1ms, showed that the jet is actually a single jet that is whipping rapidly and thus gives the impression that is splitting [44, 45, 46, 47].

1.4.2 Electrospinning parameters

1.4.2.1 Electric Field strength

Applied voltage affects electrospun fiber diameter and morphology. At the onset of applying voltage and gradually increasing it causes fiber diameter to enlarge. A low value of applied voltage causes defects that is bead formation as well as very high values. Therefore it is imperative to find the optimal range. Deitzel et al. investigated the effect of applied voltage on the polyethylene oxide (PEO)/water and found that an increase in voltage caused a change in between the pendant drop and the Taylor cone. At low values, pendant drop is formed and at the tip Taylor cone is formed. As the field strength is increased, the volume of the pendant drop shrinks and the Taylor cone emerges more and replaces the drop. When after this point, the field strength is increased even more, the formed jet is being ejected and many beads are formed instead of the fibers [45, 48].

1.4.2.2 Flow rate

Flow rate also affects fiber diameter and whether or not beads are formed. Increasing the flow rate, increases the electrospun fiber diameter. Taylor [49] found that a high flow rate causes the jet formation to be disrupted and not maintained during the electrospinning process. At high flow rates, Megelski et al also found that significant amount of beads are formed since too much solvent did not have enough time to dry before reaching the collector [50].

1.4.2.3 Collector Distance

The collector distance is another parameter that affects fiber diameter and morphology. This distance actually distinguishes whether or not there is electrospinning or electrospraying. A short distance causes an electrospin setup to start electrospraying. Increase in collector distance causes to have a smaller nanofiber diameter as also found by Doshi and Reneker. Jaeger et al. found that fiber diameter decreased from 19 to 9 μm after traveling a distance of 1 and 3.5 cm respectively. Megelski *et al*. showed that a shorter collector distance does not give enough time for the solvent to evaporate and it leads to bead formations [50].

1.4.2.4 Solution Concentration

The solution concentration determines whether the polymer is able to be electrospun or not. A too diluted solution will not electrospin and solution will break into droplets due to surface tension effects. In contrast, a higher concentrated thus viscous

solution cannot be electrospun either. Therefore an optimal concentration range is required. Within the optimal range, increased polymer concentration caused nanofibers diameter to enlarge. Doshi and Reneker found that for PEO/Water solution works viscosity range of 800-4000 centipoises [51].

1.4.2.5 Solvent Volatility

The solvent volatility is important due to the fact that fiber jet travels toward the grounded collector and a phase separation occurs between the solvent and solid polymer. A sufficiently volatile solvent will evaporate and allow solid polymer nanofiber to be deposited onto the collector. Additionally, the solvent volatility affects microtexture of the electrospun nanofibers. The pores formed on the nanofibers increase the pore density in the nanofiber mat. Megelski et al examined the effects of N,N-dimethylformamide (DMF) and tetrahydrofuran (THF) on polystyrene nanofibers. 100% THF which is more volatile than 100% DMF was used as the solvent for polystyrene solution and it gave higher density of pores and increased surface area of nanofibers [50].

1.4.2.6 Solution Conductivity

Solution conductivity affects the fiber diameter due to the fact that the polymer solution carries charged ions. A higher conductive solution will experience a higher electric force and cause fiber diameter to be smaller. Zhang et al investigated the effects of adding NaCI into the Polyvinyl alcohol (PVA) / Water solution. By increasing the NaCI concentration from 0.05% to 2% the mean fiber diameter decreased from 214 ± 19

nm to 159 ± 21 nm. Jiang et al. observed that after adding bovine serum albumin (BSA) into the dextran solution, the electrospun dextran nanofibers had a decreased mean diameter from 2.5 μm to 500 nm [53].

1.4.3 Tissue Engineering

Electrospun nanofibers offer to deal with several tissue engineering problems in vascular, bone, tendon/ligament and neural tissues. Parameters to consider when dealing with tissue engineering applications are the choice of the material, fiber orientation, porosity, surface modification and fiber morphology. Synthetic and natural or a hybrid material can be chosen. Whether the electrospun nanofibers are random or aligned in a direction has an effect on tissue response as well as the porosity which allows cell infiltration. Surface modification is another advantage that enhances cellular attachment and activity.

1.4.3.1 Material Choice

The material chosen for tissue engineering must be biocompatible that is should not be toxic and not induce at all or very little inflammatory response in the host tissue. In other words, it should be bionert. Synthetic materials are divided into two whether they are biodegradable or non-biodegradable. Biodegradable materials offer the advantage of not needing a second surgery to remove the implant. In addition, the degradation can be controlled to match tissue regeneration rate by varying material parameters. Kim et al. showed that by varying the polymer blending ratio of poly (lactide) (PLA), poly (lactide-

co-glycolide) (PLGA), poly (lactide-b-ethyleneglycol-b-lactide) (PLA-b-PEG-b-PLA) and free lactide, degradation rate of the blend could be controlled [54]. It is also imperative that the degradation rate should be matching tissue regenearation rate. A faster degradation rate will yield a mechanically less stable tissue whereas a slower degradation rate will not allow sufficient tissue formation. Non-biodegradable materials are also electrospun. Kenawy et al. electrospun poly(ethylene-co-vinyl alcohol) (EVOH) nanofiber mats and were able to culture smooth muscle cells and fibroblasts in these scaffolds [55].

There has also been research on electrospinning natural materials since these are natural materials forming the ECM. Collagen, chitosan, gelatin, fibrinogen and hyaluronic acid are some of them. However, these natural biomaterials are difficult to electrospin or their physical properties are not meeting the scaffold requirements. Therefore, a blend of natural and synthetic materials is an alternative electrospinning option. Stitzel et al. blended type I collagen (45%), PLGA (40%) and elastin (15%) to form a vascular prosthesis by electrospinning. The blended prosthesis which was more stable against burst pressures showed enhanced mechanical properties due to the addition of PLGA, and also showed compliance similar to native vessel structure [56].

1.4.3.2 Fiber Orientation

Electropspinning provides the opportunity to have random or aligned fibers. Random fibers are formed on a stationary collector whereas aligned fibers are collected on a rotating mandrel. Anisotropy is required in vivo in certain tissues. Xu et al

electrospun aligned nanofibers of poly (L-lactate-co-e-caprolactone) (P(LLA-CL)) (75:25) and used tissue culture polystyrene and solvent cast (P(LLA-CL)) films as the controls [57]. They seed human coronary artery smooth muscle cells onto the scaffolds and observed that smooth muscle cells attached and oriented in the direction aligned nanofibers. In addition, cells had improved adhesion and proliferation compared to the controls. Schnell et al. examined the axonal outgrowth and glial cell migration on aligned collagen/ poly (e-caprolactone) (PCL) nanofibers. They found that the blended polymer allowed superior axonal guidance than the individually electrospun nanofibers [58]. Cooper et al. [59] demonstrated that chitosan-PCL blend af aligned nanofibers supported a neuron-like cell PC-12 adhesion and had increase growth along the aligned fiber direction. They also examined β-tubulin gene expression which is a marker for neuronal extensions and found that PC-12 cells on aligned nanofibers had increased β-tubulin gene expression than the ones on random nanofibers.

1.4.3.3 Porosity/Pore size

Eichhorn and Sampson examined mean pore radius of electrospun fiber scaffolds. They showed that 100 nm diameter nanofibers with a 80% porosity had a mean pore size of 10 nm. They also demonstrated that for a given areal density and porosity, increasing the fiber diameter increases the mean pore size [60]. This is a paradox that in order to increase the surface area the diameter of the fibers need to be smaller; however the mean pore size decreases as well. The decreased pore size makes the scaffold essentially a two

dimensional (2D) scaffold that does not allow cell infiltration. Given that, there are cases in which cell infiltration is unwanted and a 2D layer is desired. Skin and endothelium are examples for this case. A 2D scaffold made with electrospun nanofibers provides high surface area for endothelial cell attachment and at the same time prevents smooth muscle cell migration into this area as is the case in vivo.

When a 3D structure is required such that cell infiltration into the matrix is desired, the pore size needed is around 10 μm for cells to infiltrate through. Li et al. electrospun highly porous (92%) nanofibers with the diameters 500-800 nm [61]. The pore size was 2-465 μm and they seeded this scaffold with C7 mouse fibroblasts. Cells proliferated on this scaffold 5 folds and after three days cells start to migrate to underlying layers forming a 3D cellular structure.

1.4.3.4 Surface Modification

Cellular attachment can be enhanced by functionalizing the electrospun nanofibers surface. RGD is a peptide sequence that when nanofiber surface is functionalized with it, integrin on cells recognize and bind to it . Kim et al. observed that RDG treated surfaces enhance cellular (NIH3T3) attachment, spreading and proliferation [62].

1.4.3.5 Controlling Nanofiber Morphology

In section 1.4.2, we have discussed electrospinning paramaters to control nanofiber morphology. In addition to those, electrospun nanofibers offers encapsulation

of nanoparticles that contain biological active molecules. Wnek et al encapsulated endothelial growth factor which is fluorescently labeled with Alexafluor 488 (green) and separately bovine serum albumin which is labeled with Texas-Red (red) into PVA nanoparticles. They then electrospun the polymer solution containing PVA nanoparticles and obtained distinct domains of bioactive molecules in nanofibers [63, 64]. This has great advantage of being able to release certain compounds at different rates and times which is desired for neural tissue engineering where different sets of biological cues are required.

1.4.3.6 Bone tissue engineering

Electrospun nanofibers has also use in bone tissue engineering. Thomas et al examined the mechanical properties of aligned PCL nanofibers to be apllied to bone tissue. With different rotation speeds, they found the aligned nanofibers mechanical properties vary [65]. When the rotation speed is 0 RPM, the tensile strength was 2.21 ± 0.23 MPa and the tensile modulus was 6.12 ± 0.8 MPa whereas when the speed was increased to 6000 RPM, the tensile strength increased to 9.58 ± 0.71 MPa and the tensile modulus increased to 33.2 ± 1.98 MPa.

1.4.3.7 Tendon/Ligament tissue

Tendon and ligament repair is another area where electrospun polymer nanofibers can be utilized. Tendon and ligament have relatively high tensile strength and therefore in a scaffold collagenous connective tissue formation is essential. Quyang et al knitted

PLGA scaffold for regenerating a 10 mm gap in Achille tendon of a rabbit. After two weeks of the scaffold implantation, they observed that type I and III collagenous connective tissue was regenerated and after 12 weeks, tensile modulus and stiffness of the implant reached 50% of the normal tendon tissue [66].

1.5 Neural Tissue Engineering

Peripheral nerve injury due to traumas may lead to sensorimotor defects because of not having a sophisticated repairing technique. Clinically, the injury is either coaptated from the transected part or if there is a large defect, an autograft is used. An autograft from the patient transplanted into the defective site can give functional recovery however this solution has drawbacks such that the donor site has limited availability and possible loss of function at the donor site. An alternative solution is the allograft which is a transplant from another human being or an animal. However, this technique causes immune problems at the host site. Therefore, artificial nerve guidance conduits (NGC) is a solution to this clinical problem that it can guide the axon and regenerate the defective nerve [63].

Examples for synthetic NGCs are microchannels, microfibers and hollow fiber membranes. These have advantages of increased availability, not needing a surgery for the donor site and better fixing of the axon at the suture site. NGCs have shown great promise *in vitro* but it is difficult to direct axon and regenerate nerve *in vivo*. In addition NGCs cannot respond to a nerve defect which is above a critical length. NGCs cannot

selectively guide sensory or motor axons toward the end organs and due to their rigid structures there are issues of handling during the operation and implantation.

Electrospun nanofibers due to their nanoscale feature size, fibrous morpghology mimicking ECM, being functionalized with or encapsulating bioactive molecules and anisotropic properties offer superior advantages over previous techniques. NGCs made of electrospun nanofibers (random or circumferentially aligned) can be fabricated either on a rotating mandrel or onto a collector that folded into a tube shape after electrospinning process. Post electrospinning allows obtaining multiple stacked layers. At the inner portion one can have aligned nanofibers whereas at the outer portion random fibers can be seen [63].

1.5.1 Differentiation of stem cells

Differentiation of stem cells is possible with biochemical, topographical and electrical cues. Recently, electrospun nanofibers, due to their nanoscale morphologies, have emerged as a tool to differentiate stem cells.

Xia et al. [67] have demonstrated that embryonic stem cells that are seeded onto aligned PCL nanofibers can differentiate into neural lineages. In addition, the neurite outgrowth was in the direction of aligned nanofibers. Results of O4 staining, which is an antibody for oligodentrocyte specific glycolipid, show multipolar morphology on the nanofibers. Oligondentrocytes migrated along the aligned nanofiber direction, which shows a possible myelination of axons. On the contrary, when the cells were seeded onto

random nanofibers, the neurite extensions were in all directions as well as the migration of oligodentrocytes.

Mao et al. [68] showed that when neural stem cells cultured in a petri dish with 1 mM retinoic acid and 1% fetal bovine serum (FBS), the neural stem cell spread and differentiated into oligodentrocytes. However, when the cells were on 749 nm and 1452 nm fibers, they differentiated into neuronal lineage. These results show that topographical and biochemical cues both affect differentiation lineage.

1.5.2 Neurite Outgrowth

Ramakrishna et al. [69] found that scaffolds made out of aligned electrospun nanofibers were better environments than random microfibers for culturing nerve stem cells. They found that aligned nanofibers were able to direct neurite extension. This was verified with Martin et al.'s work that electrospun aligned nanofibers were able to direct dorsal root ganglia (DRG) neurite growth even without any surface modification. Xia et al. [70] seeded DRG at the border of a random and aligned fiber mat. The cells responded to their environments by following the directionality of the nanofibers. The neurites on the aligned nanofibers portion were aligned in the nanofiber direction whereas the neurites at the random nanofiber portion made random extensions

In order to regenerate a nerve when using electrospun aligned nanofibers, the surface needs to be functionalized with bioactive molecules such as ECM proteins (laminin, fibronection) or growth factors (basic fibroblast growth factor (bFGF) or nerve growth factor). Li et al. [71] immobilized bFGF and laminin on PLA nanofibers so that

both physical and biochemical stimulations could occur. The immobilized biochemical factors were as efficient as the soluble ones and enhanced the neuritic growth by 2-4 fold. Surface treatment of nanofibers with plasma also affects neurite growth. In order to increase surface hydrophilicity, Ramakrishna et al. [72] plasma treated the PCL nanofibers and found that Schwann cells had increased adhesion and proliferation on the nanofibers.

Mey et al. [73] examined 25:75 collagen/PCL blend nanofibers compared to PCL only nanofibers in terms of cellular activities. They showed that schwann cell migration, neurite orientation and growth were all enhanced compared to PCL nanofibers. DRG explants had better axonal guidance on collagen/PCL blend nanofibers. These results show that blended nanofibers have superior performance compared to single polymer nanofibers. PCL improves mechanical properties whereas addition of collagen increases cellular cytocompatibility. Ramakrishna et al. [63] also found similar results that they have blended chitosan with PCL. They found that the blend had better tensile strength, higher cellular attachment and proliferation compared to either chitosan or PCL alone fibers.

Ambrosio et al. [74] examined gelatin cues on PC-12 cell nerve growth. They electrospun a blend of 50:50 Gelatin/PCL nanofibers and observed that cellular differentiation, proliferation, and adhesion were enhanced compared to PCL-only nanofibers. In addition, contact angle measurements showed a more hydrophilic behavior due to the gelatin content. Koh et al. [75] examined adding laminin to nanofibers by covalent binding, physical adsorption and blended electrospinning techniques. They

found that PC-12 cells had increased axonal extension when they are seeded onto blended laminin-PLLA electrospinning nanofibers compared to other techniques.

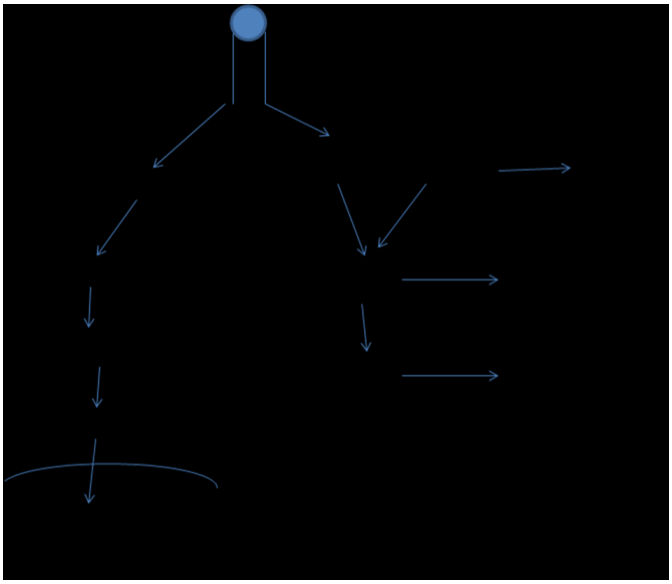

Figure 1.3 Signaling pathways for PC12 cell differentiation and neurite extension, modified from [114]

Nerve growth factor (NGF) is a key ligand for differentiation of PC12 and neural stem cells. Figure 1.3 shows known signaling pathways that enable the differentiation following the administration of NGF, including a biochemical upregulation of differentiation proteins and cytoskeletal signals for neurite extension [114]. Receptor Tyrosine kinases are transmembrane proteins with an extracellular ligand binding domain and intracellular tyrosine kinase domain. After the receptor activation by specific ligand binding, downstream pathways of Ras and the phosphatidyl inositol-3 kinase (PI3K) are

activated. The Ras- extracellular signal regulated kinase (ERK) pathway is responsible in gene transcription for differentiation. The PI3K- actin cytoskeleton pathway is responsible for neurite growth [114,115].

The growth cone generates forward tension on the elongating axon. The growth cone typically has 2 different domains: a central domain dominated by microtubules and a peripheral region dominated by actin filaments. In the peripheral domain, actin filaments undergo plus end directed assembly and elongation at the tip of the lamellipodia and filopodia, and at the same time push the cone membrane in the forward direction. Simultaneously, actin filaments are dragged back to the central region to depolymerize (retrograde flow), leading to equilibrium. Retrograde flow prevents microtubules from going into the peripheral domain. Surface adhesive ligands shift the balance towards polymerization for neurite extension, through a lack of retrograde flow, causing the axon to extend [118].

In addition to growth factors, ECMs like laminin and fibronectin also play a role in both *in vitro* and *in vivo* axonal growth. Integrins are the family of cell surface receptors for the amino acid ligand sequences in ECM proteins. ECMs do not induce neurite elongation when NGF is not supplied. Instead, ECM-integrin coupling increases the effects of growth factors. There is a cross talk between integrin signaling and growth factor signaling pathways. This cross talk can be in the form of either directly phosphorylating the growth factor receptors, or in the form of a gene expression [116]. Dikic et al. demonstrated this by seeding PC12 cells on plastic and laminin coated dishes and comparing their responses to growth factor stimulation. Cells without the epidermal

growth factor (EGF) did not survive, whereas cells on laminin coated dishes did. When EGF was supplied to the culture, cells on plastic dishes had minor neurite elongations, whereas cells on laminin had rapid neurite outgrowth. They found that Pyk2/FAK complex regulated neurite outgrowth and acted as a linker between the integrin and growth factor signaling pathways [117]. Alvarez-Perez et al. seeded PC12 cells onto Gel/PCL blend of electrospun polymer nanofibers. Compared to a PCL nanofiber control, they reported increased differentiation and increased growth associated protein (GAP-43) at the growth cone due to the incorporation of gelatin. They suggest that gelatin mediated integrin receptor could be in cross talk with the tyrosine kinase receptor signaling pathway to effect PC12 cell differentiation. GAP-43 was enriched at the interface of receptors and cytoskeleton, which could play a role in initiated extension of the actin cytoskeleton of the growth cone tip [104].

1.5.3 Repairing peripheral nerve defects

Given the success of electrospun nanofibers *in vitro*, they also show a great promise when used for repairing nerve injuries and regenerating axons *in vivo*. Ramakrishna et al. [76] showed that 5 out of 11 NGCs made of PLGA electrospun random nanofibers were able to regenerate a 10 mm nerve defect. Gelain et al. were also able to regenearate a 10 mm nerve defect with random nanofibers made a blend of PLGA and PCL. These nanofibers were not coated with any bioactive molecule. This shows that only by topographically electrospun nanofibers were able to regenerate nerve defect. In addition, Gelain et al. were able to record electrical impulses from the distal end. Therefore, NGCs not only extending axons but also facilitating the re-innervation of nerves.

Most of these nanofiber based NGCs are randomly electrospun. Leong et al. [77] fabricated NGCs made of axially aligned nanofibers to examine the effect of alignment on nerve regeneration. NGCs were fabricated by rolling and sealing a non-woven nanofiber mat. They were able to regenerate a nerve with 15 mm defect which was superior compared to random fibers. In these conduits, however, the outer layer is a film that hinders nutrient and waste exchange. Instead, Pandit et al. [78] showed recently that nerve conduits can be made of multi layers such that at the outer layer there is a random thick mat which provides the mechanical strength and due to porous structure allows freely nutrient and waste exchange. In the interior layer, there is axially aligned nanofibers that facilitate axonal outgrowth and regeneration [63].

1.6 Conclusions

In order to better diagnose and develop therapeutics for neurological disorders, it is important to better understand the underlying mechanisms of neurological disorders and thus conducting research on neuronal networks is one way of seeking cures for these disorders. However, complexity of the neuronal networks makes this task difficult and therefore a solution to this problem is to simplify and organize neuronal networks by cell patterning using microfabrication techniques. Electrospun polymer nanofibers proved to be a good candidate for many tissue engineering applications due to the ECM-like structure. Ongoing research and progress in microfabrication and electrospun nanofibers make them good candidates for potential tools of seeking cures to neurological disorders

CHAPTER 2: CONFINED NEURAL NETWORK DEVICE DESIGN AND FABRICATION

2.1 Introduction

Our device for micropatterning neuronal networks is in the form of a grid pattern and the first step for fabricating the device is transferring the grid pattern from a chrome mask onto a silicon wafer using photolithography. Next, PDMS is poured onto the wafer and after it is cured the negative replica is peeled off the from the master template. Polystyrene (PS) dissolved in anisole is spin coated onto this newly peeled of PDMS mold. After removing the excess polymer from the raised features, the polymer pattern is transferred onto the already electrospun Gel/PCL nanofibers using double stamp micromolding technique.

2.2 Materials and Methods

2.2.1 Device Geometry

Our device geometry for micropatterning neuronal networks on nanofibers platform embraces a rectangular grid shape. The grid is formed with the nodes that are interconnected to each other by lines. The rectangular grid shape allows to study neuronal

elongations in two different line lengths and directions. The nodes in the center of the interconnecting lines provides the location for cell body. The lines are 3 µm wide and the node has a diameter of 15 µm. From the center to center of the neighboring nodes, the longer dimension of the rectangular grid is 45 µm whereas the shorter dimension is 30 µm. We call this device Confined Neural Network (CNN) to imply that the cell body is confined to a node and the cell is allowed to make connections with the neighboring cell only by extending its neurites. A scheme of CNN is shown in figure 2.1 below.

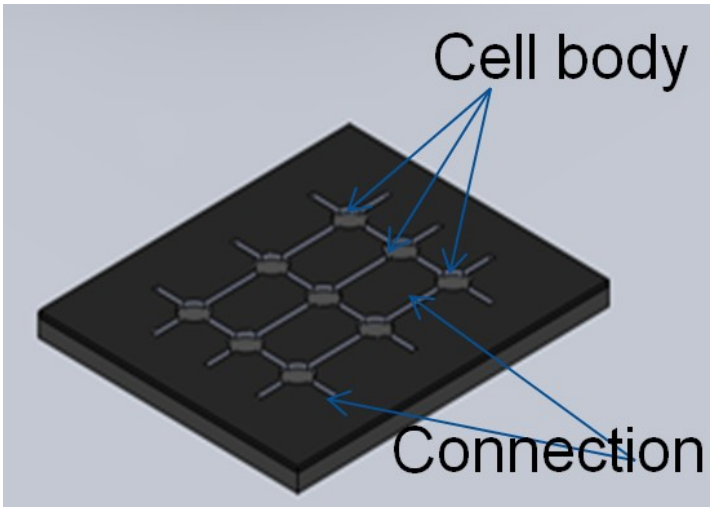

Figure 2.1 Confined Neuronal Network (CNN)

2.2.2 Silicon Wafer Patterning

The master template for the CNN pattern is a silicon wafer and is fabricated and patterned using photolithography. Cleaning of the silicon wafer is essential for patterning the negative photoresist (SU8) on it. A piranha solution which is a mixture of 3:1 sulfuric acid (H_2SO_4) and hydrogen peroxide (H_2O_2) is used for cleaning. The silicon wafer is

immersed into piranha solution for 15 minutes at 120 ^{o}C and rinsed with Deionized (DI) water. Next, the wafer is heated at 150 ^{o}C for 5 minutes to get rid of residual water on the surface. This dehydration step is necessary to increase adhesion of the photoresist features to the wafer. SU8 2005 is spin coated on the wafer at 2500 RPM to get 5-6 µm high features. The wafer is then soft baked at 95 ^{o}C for 2 min to get rid of the residual solvent. EV 620 contact aligner is used to expose the photoresist to UV for 6.5 sec. The mask for the pattern is made out of chrome printed on a glass frame. After UV exposure, SU8 needs a post exposure bake to complete the cross linking.

A post exposure bake of the wafer at 95 ˚C for 3 min is performed. After post exposure bake a latent image of the pattern is seen on the photoresist. Next, the wafer is immersed in SU8 developer and agitated for 1-2 min. The wafer is then washed with fresh SU8 developer and rinsed with isopropyl alcohol (IPA) and air dried. The pattern is checked under an inspection microscope to confirm the successfully patterned features. A micrograph of the patterned silicon wafer is shown in figure 2.2 (A) below.

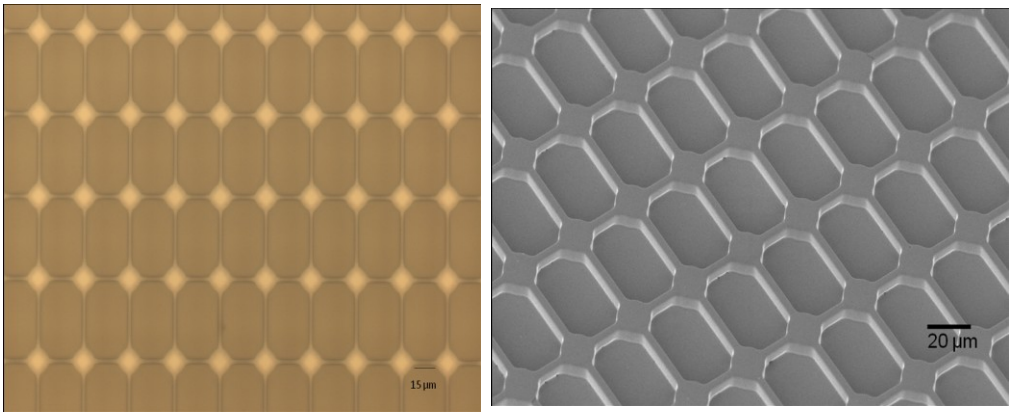

Figure 2.2 (A) Patterned Silicon Wafer (B) SEM image of the PDMS Mold

2.2.3 PDMS Molding

A negative replica is needed for double stamp micromolding technique. T-2 translucent PDMS is mixed with 10:1 its curing agent. The mixing takes place rigorously for 5 min and bubbles form within the mixing cup due to the air being trapped during mixing. A vacuum desiccator is used to remove the bubbles. Cycling on and off the vacuum drives off the bubbles and allows to obtain a bubble free mold. The mixture is then poured ~ 70 gr onto the silicon wafer which is in a 4 inch PS petri dish and allowed to cure for 48 hours at room temperature. An SEM image of the mold is shown in figure 2.2 (B).

2.2.4 Electrospinning Gel/PCL nanofibers

Gelatin 6.7 wt% in hexafluoroisopropanol (HFIP) was blended 20:80 with PCL 5 wt% in HFIP. The blended solution is then put into a 20 cc syringe with a 20 GA dispenser. Positive 25KV was applied to the metal tip. A metal ring is also attached to the tip to guide the electric field. Grounded metal with an area of 3X3 square inches was covered with aluminum sheet to collect the electrospun nanofibers. The solution was electrospun at a distance of 20 cm from the tip to the collector. A syringe pump is used to control flow rate. The flow rate we have used for 20:80 Gel/PCL nanofibers was 15 ml/hr.

2.2.5 Mictotransfer Molding

Microtransfer molding which is initially developed by Whitesides et al. is a type of micromolding technique [79]. In this technique microstructures are formed by filling the microchannels on a PDMS mold with a liquid pre-polymer. Excess polymer is scraped by a flat piece of PDMS and then the mold is brought into contact with the flat substrate and prepolymer is cured with exposing it to either heat or UV. After curing, PDMS mold is peeled off and thereby leaving cured polymer microstructures on the substrate. There are many advantages of this technique. It is rapid and can generate patterns in five minutes. It is able to provide both isolated and interconnected patterns. It can be used for fabricating three dimensional structures and can be patterned on contoured substrates. It does not have to be restricted to small areas as it is the case in photolithography. A large area pattern is possible using this technique. Whitesides et al. have reported 3.5 cm long channels that are patterned with microtransfer molding. Another advantage is that this technique can be applied to many different substrates such as Si, SiO_2 and Au. However, one limitation of microtransfer molding is thin film produce in between raised features. This film is due to transfer of polymer from the raised features of the pattern or some leaking of the fluid from the capillaries. This residual film can be removed with oxygen plasma treatment however this introduces additional cost and fabrication steps [79].

2.2.6 Double stamp micromolding technique

Double stamp micromolding technique is a modified version of the microtransfer molding. In this technique, the residual thin film left in between features of pattern during microtransfer molding has been taken care of. This process allows to fabricate individual microstructures successfully and is adapted from work of Guan et al [80,81]. A polymer is spin coated onto the PDMS mold that has the desired pattern. The mold is first contacted to a planar substrate with lower pressure, thereby removing the polymer from the raised features. Next, the mold is stamped to a substrate with a higher pressure that transfers the polymer from the recessed features to the substrate [5].

During double stamp micrmolding technique, the phenomena called "dewetting" is utilized. Dewetting is the spatial separation of the thin polymer film due to the instabilities at the liquid-air interfacial layer. These instabilities can be physical, chemical or thermal [82, 83] Dewetting is the rupture of the polymer film and become droplets on the surface. Karim et al. [83] have modified silicon surface using microcontact printing and patterned SAMs of octadecyltrichlorosilane (OTS) . After spin coating polystyrene (PS) solution dissolved in toluene , they were able to obtaine a micrometer scale dewetted pattern of PS fims. Ferrell, N and Hansford, D have obtained spin dewetting of PS solutions up to 20 % (w/w) on a topographically patterned PDMS mold. By combining soft lithography and spin dewetting on a topographical mold, they were able to obtain thin films of <100 nm and thick films of >5 μm. By altering the polymer concentrations, different phases of dewetting were obtained. Complete dewetting required a relatively low level of polymer concentration (0.125-3%) whereas a higher concentration (20%)

formed a fully covered non-dewetted film. During complete dewetting, there is no polymer at the raised features of the PDMS pattern. A partial dewetting (5-15%) is where the polymer on the raised features is ruptured from the polymer on the recessed feature. This process is purely topographical and therefore there is no need for any surface chemical treatment. Topographical features cause dewetting during spin coating process [84].

2.2.7 Stamping of the CNN

After having the PDMS mold for the CNN device, we spin coat a polymer solution onto it and transfer this polymer pattern onto the electrospun nanofibers using heat and pressure.

A 9% PS solution is dissolved in anisole for spin coating. The polymer solution is spin coated at 3000 RPM and we get dewetting on the mold. The excess polymer on the raised features of the mold is removed by contacting the mold to a glass slide at 100 ^{o}C with 0.5-2.5 psi.

The raised features on our mold are the CNN pattern with nodes that are interconnected to each other with lines. Since we remove the polymer from this feature by dewetting and contacting the excess polymer to a glass slide, we then get holes instead of nodes and grooves instead of lines on the PS film which sits on the PDMS mold. 8 wt% polyvinyl alcohol (PVA) dissolved in deionized (DI) water and applied to the mold. After the PVA film is dried, it is peeled off. The next step is to transfer this PVA standing

PS pattern onto the nanofibers. PS pattern is transferred onto the nanofibers at 52-54 ^{o}C with applying 100-150 psi.

2.3 Results and Discussions

Figure 2.3 (a-h) shows the process layout for fabricating the CNN device after the mold is ready. After patterning silicon wafer, PDMS mold which is the negative replica of the pattern is obtained. PDMS mold allowed us to use double stamp micromolding technique. After dewetting and removing excess polymer on the raised features, the grid PS pattern on the mold is transferred onto electrospun Gel/PCL nanofibers using heat and pressure.

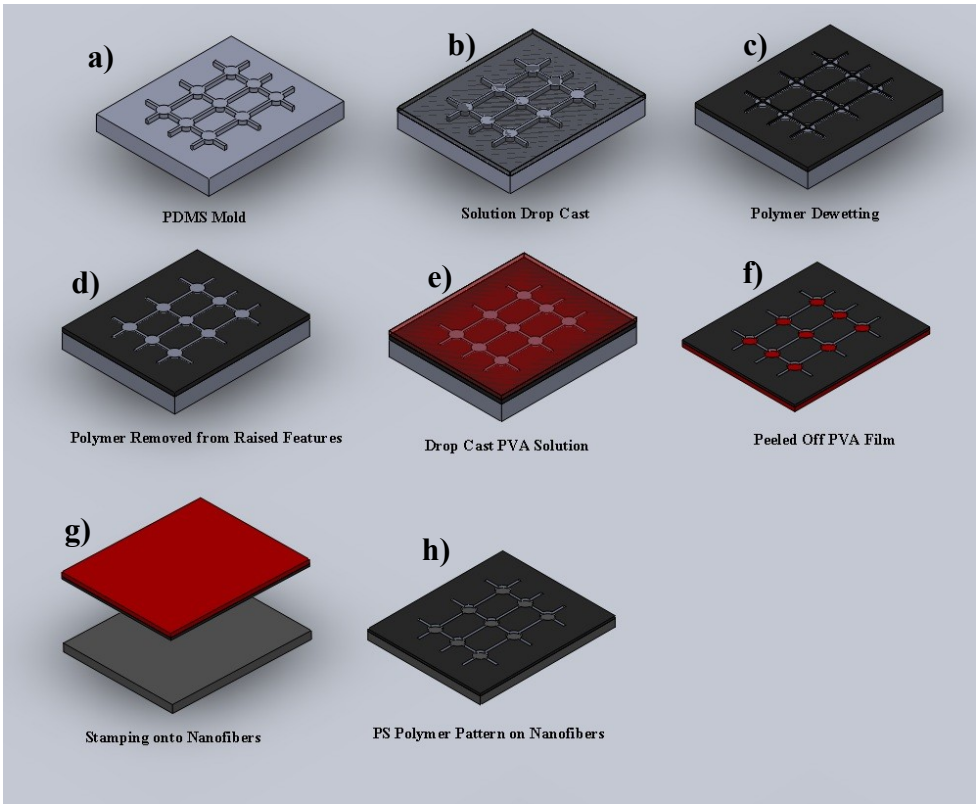

Figure 2.3 Fabrication steps of the CNN device

2.4 Conclusions

In this chapter we discussed fabrication of the CNN devices. A PDMS mold is obtained with soft lithography after patterning a silicon wafer using photolithography. PS grid pattern from the PDMS mold is transferred onto electrospun polymer nanofibers using heat and pressure.

CHAPTER 3: MICROPATTERNING NEURONAL NETWORKS ON ELECTROSPUN RANDOM NANOFIBERS

3.1 Introduction

Recently there has been increasing demand to better understand how biological neural networks process and store information. The complexity of mammalian brain led researchers to study the in vitro cultures since they possess relatively reduced connections. However, these cultures are randomly organized and their neurites overlap making synaptic coupling studies extremely difficult [85]. Therefore, there is a need to guide neuronal connections and their spatial development [86].

Cell patterning has proven important in studies of cell properties [87], guidance and adhesion [88]. It has also allowed researchers to study biocompatibility of variety of substrates [89, 90] cell based biosensors [91] and tissue engineering applications [92].

There are two major strategies for cellular patterning; chemical and topographical. Chemical patterning modifies surface chemistry and creates cell adhesive regions on a repellant background. Lift off and microcontact printing are widely used methods for chemical modification of surfaces. Micropatterns are produced photolithographically onto a silicon wafer and incubated with adhesion proteins. Photoresist is then lifted-off leaving cytophilic regions [93, 94]. Microcontact printing allows a wide range of

biomolecules to be patterned onto a solid background [95]. An adhesion promoting ink solution is applied onto an elastomeric stamp and transferred onto a substrate by stamping.

Topographical patterning can be produced on glass (or silicon) by the photolithography and reactive ion etching techniques. Surface topographic grooves guide neuronal network geometrically [96] and field of silicon pillars affect growth of neurons [97].

Recently, electrospinning has emerged as a versatile technique that allows to create fine fibers made of synthetic and natural polymers mimicking the extracellular matrix (ECM) [98]. Electrospun nanofibers have high porosity and surface to volume ratio which is highly advantageous for tissue growth [99]. Nerve cells could attach, proliferate and extend neurites on polycaprolactone (PCL) based nanofiber scaffolds [100] and showed important evidence of cellular morphology to spread bipolar elongations [101]. A blend of synthetic and natural polymers is more attractive since synthetic polymers have good mechanical properties whereas natural polymers have better cellular affinity [102]. Incorporation of gelatin (Gel) a natural polymer into PCL nanofibers enhances nerve proliferation and differentiation [103] and all fundamental aspects of nerve regeneration [104]. In order to further enhance interaction of cells with scaffolds, nanofibers can be modified with ECM proteins [105]. Collagen is the major component of the ECM and because of its excellent biocompatibility, it enhances cellular attachment and viability [106, 107] as well as promoting the neurite outgrowth [108].

Cells in previous works are patterned on solid substrates, which have to go through harsh solvents and lack in vivo characteristics. In contrast to these substrates, in this paper, we fabricate a device which patterns neuronal cells on collagen coated ECM-like electrospun Gel/PCL nanofibers using microfabrication techniques. In addition, on our devices, the cellular attachment, viability and differentiation of neuron-like PC12 cells are examined.

3.2 Materials and Methods

3.2.1 Materials

PCL (Mw = 65,000) , porcine gelatin type A and PS (Mw = 350,000) were obtained from Sigma-Aldrich Inc. Rat pheochromocytoma cell-line, PC12 was obtained from American Type Culture Collection (ATCC) and mouse 2.5S nerve growth factor (NGF) was obtained from Promega Corp.

3.2.2 CNN Device Fabrication

A negative photoresist SU8 2005 was spin coated onto silicon wafer with 3000 RPM. A grid pattern of recessed features (line width, 3 um; node diameter, 15 um) on a chrome mask was transferred onto photoresist by ultraviolet (UV) photolithography. Polydimethylsiloxane (PDMS) was mixed with 10:1 curing agent and poured onto silicon master. After curing at room temperature for 2 days, negative replica was peeled off.

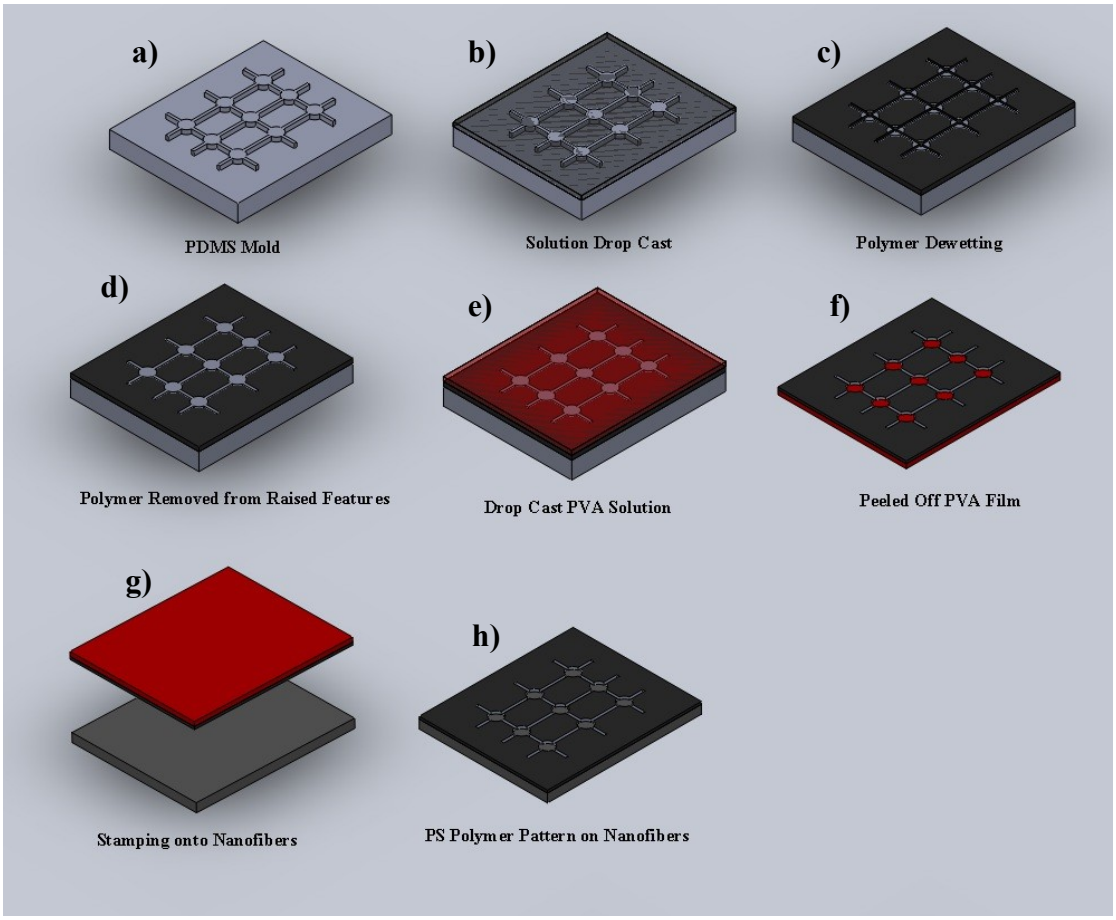

Figure 3.1 Fabrication of the CNN Microdevice

CNN microdevices are fabricated through a modified version of double stamp micromolding technique [109]. 11 wt % polystyrene (PS) dissolved in anisole was drop cast and spin coated at 3500 RPM onto the PDMS mold (Figure3.1 (a-b)). Polymer dewetted [109] (Figure 3.1c) and excess polymer on the raised features was removed by pressing onto a glass slide at 100 ^{o}C (Figure 3.1d). 8 wt% polyvinyl alcohol (PVA) dissolved in deionized (DI) water and applied to the mold (Figure 3.1e). After 1 day at

room temperature, water is evaporated from the PVA solution and the mold is annealed for 1 min at 150 ^{o}C. The mold is cooled down for 15 minutes and PVA film is peeled off from the PDMS mold and thereby also peeling off the PS features from the mold (figure 3.1 (f)). Next, PS features standing on the PVA film is stamped onto the nanofibers at ~50 ^{o}C with applying ~100 psi (Figure 3.1 (g)). Stamped nanofibers are then soaked in DI water for 1 hr for PVA film to dissolve and leaving PS features transferred onto the collagen coated nanofiber mat (Figure 3.1 (h)).

3.2.3 Fabrication of Electrospun Nanofibers

Gel 6.7 wt % in 1,1,1,3,3,3-hexafluoro-2-propanol (HFIP) and PCL 5 wt % in HFIP solutions are prepared separately by stirring them overnight at room temperature. The Gel and PCL solutions are then blended with 20:80 weight ratio and stirred for 1 hr. In a chemical hood, the blended solution is placed into a 20 cc syringe and was electrospun onto a rotating mandrel collector covered with aluminum sheet, using high-voltage DC power supply. Distance to the collector was 20 cm and the collector was set to -6kV, controlled by a motor and was rotating at 300 rpm at all times. Electrospun nanofibers are produced in 2 sets of electrospinning parameters. First, the solution was fed with 15 ml/hr for ½ hr through 20 G blunt tip and the applied potential was set to 20kV. Second, the solution was fed with 1 ml/hr for 3/2 hr through 25 G blunt tip and the applied potential was set to 13kV. Nanofibers were then kept in vacuum oven overnight for the remaining solvent to evaporate.

3.2.4 Collagen Coating onto Electrospun Nanofibers

Electrospun nanofibers were treated with oxygen (O_2) plasma for 1 minute in an inductively coupled plasma cleaner. The radio frequency (RF) power was set to 50 W and the flow rate was set to 30 sccm. O_2 plasma treated nanofibers are then immersed into the collagen solution of 300 μg/ml in 0.02 N Acetic Acid (AA) overnight at 4 ^{o}C. Scaffolds are then first washed with Phosphate Buffered Saline (PBS) for 5 min and secondly, 5 min with DI water and finally are air dried.

3.2.5 Characterization of the Electrospun Nanofibers and the Fabricated CNN Device

Electrospun nanofibers and the fabricated CNN microdevice are coated with a thin Au-Pd layer using a sputter coater and then characterized with scanning electron microscopy (SEM) operating at 5 kV. The electrospun nanofibers diameter is measured based on the SEM micrographs (n=5) using an image analysis software (imageJ; National Institute of Health, Bethesda, MD). Gelatin content of the scaffolds is confirmed previously [110].

3.2.6 Vacuum Assisted Cell Seeding

For all experiments, all of the electrospun nanofiber based samples are cut into 23x23 mm^2 and are immersed in 70 % Ethanol (v/v) for 1 hr, washed with PBS 3 times and air dried. Sterilized 10 mm diameter PDMS rings applied with high vacuum grease

are placed on all samples. Vacuum assisted cell seeding [111] with a vacuum pressure of 5-10 in Hg is used on the samples needing it.

3.2.7 Sample Types

Five types of sample are used:

1) Fabricated CNN Microdevice seeded with Vacuum Pressure (device)

2) Fabricated CNN Microdevice seeded without vacuum (nonvacuum)

3) Collagen coated random Get/ PCL electrospun nanofibers mat with cells seeded with vacuum pressure (collagen_fiber)

4) Random Gel/PCL electrospun nanofiber mat (no collagen coating) with cells seeded with vacuum pressure (noncollagen)

5) Collagen coated tissue culture polystyrene (TCPS) as a control.

10 mm diameter PDMS rings are sealed onto tcps wells of a 12 well plate. Collagen solution is applied overnight onto tcps at room temperature and washed 3 times with sterile PBS.

3.2.8 *In Vitro* Cell Culture

A neuronal cell line, PC-12 cells were cultured in 75 cm^2 tissue culture flasks at 37 ^oC and 5% CO_2. Their media was RPMI 1640 (ATCC) with supplements of 10 % Horse Serum, 5% Fetal Bovine Serum, 1% Penicillin/Streptomycin (Complete Medium). The passage number of PC12 cells were kept at 10-20 for all experiments. Cells are

seeded onto all samples with a density of 73800 cells/cm^2 for all experiments and 0.2% Amphotericin B is added to all experimental cultures.

3.2.9 Cell Adhesion Assay

Alamar Blue assay (Invitrogen) is used to measure metabolic activity of cells which directly correlates to the number of adhered cells. Samples are cultured in 12-well plates and in complete medium for 4 hr . PDMS rings are removed from the culture and all samples are washed 2 times with PBS and incubated for 3 hr in dark in fresh complete medium which is mixed with Alamar Blue assay (Invitrogen) reagent 10:1. Aliquots were pipetted into wells of a 96-well plate to be analyzed with a spectrophotometric plate reader . The fluorescence at 590 nm for each well was recorded and results are normalized to TCPS.

3.2.10 Cell Viability Assay

Cell Viability of the samples in 12-well plate were analyzed by Alamar Blue assay after 1 and 3 days of culture with the complete medium changing every other day. After 1 day, PDMS rings are removed from the culture. At the end of the prescribed time samples are washed with PBS and incubated for 3 hr in dark in fresh complete medium which is mixed with Alamar Blue assay reagent 10:1. Aliquots were pipetted into wells of a 96-well plate to be analyzed with a spectrophotometric plate reader . The fluorescence at 590 nm for each well was recorded and results are normalized to TCPS.

3.2.11 Immunoctyochemistry and Neurite Length

For differentiation studies samples are cultured in 12-well plate and after the first 6 hr, samples are washed with PBS and they were put back into fresh complete medium containing 100 ng/ml Nerve Growth Factor (NGF). After the first 12 hr, the culture medium is changed to RPMI 1640 Medium, 1% Horse Serum, 1% Penicillin/Streptomycin and 100 ng/ml NGF (Differentiation Medium). The differentiation medium was changed every other day.

After 4 days PDMS rings are removed from the culture, samples are washed with PBS and fixed with 4% paraformaldehyde for 15 min at room temperature followed by permeation with 0.3% Triton X-100 in PBS. Samples are washed 3 times with PBS for 5 min each and immersed in 5% Bovine Serum Albumin (BSA) in PBS for 1hr to block non-specific labeling. Samples are stained with anti-beta-tubulin monoclonal antibodies (1:500, Millipore) overnight at 4 ^{o}C. Samples are washed 3 times with PBS 5 min each and incubated in alexa fluor 546 conjugated donkey anti-mouse secondary antibodies (1:50) at 37 ^{o}C for 1hr in dark. Samples are washed 3 times with PBS for 5 min each and actin filaments were stained with Alexa Fluor 488 labeled phalloidin (Invitrogen) for 30 min at room temperature followed by 3 times PBS wash 5 min each and counterstained with 4',6-diamidino-2-phenylindole dilactate (Dapi, Invitrogen) for 5 min. Samples are washed 3 times with PBS for 5 min each and viewed by Nikon Ti Microscope. 10 Random fields per sample at 20x lens were collected. The number of differentiated cells was determined by having at least one neurite equal to or greater than 5 μm in length and was reported as the percentage of total number of cell nuclei in the field. Neurite length

was measured with ImageJ. If a neurite had branches, the branch length was calculated from the branching point.

3.2.12 Statistics

All data presented are expressed as mean ± standard deviation (SD). Results were subjected to unpaired student's *t*-test for statistical significance analysis ($p < 0.05$). Each parameter was conducted in triplicate (n=3) samples.

3.3 Results and Discussions

3.3.1 Fabricated CNN Microdevice

SEM micrographs of the device fabrication process and the final CNN microdevice on nanofibers platform are shown below (Figure 3.2). The fabricated microdevice had ~5 um groove widths and ~18 um diameter of wells.

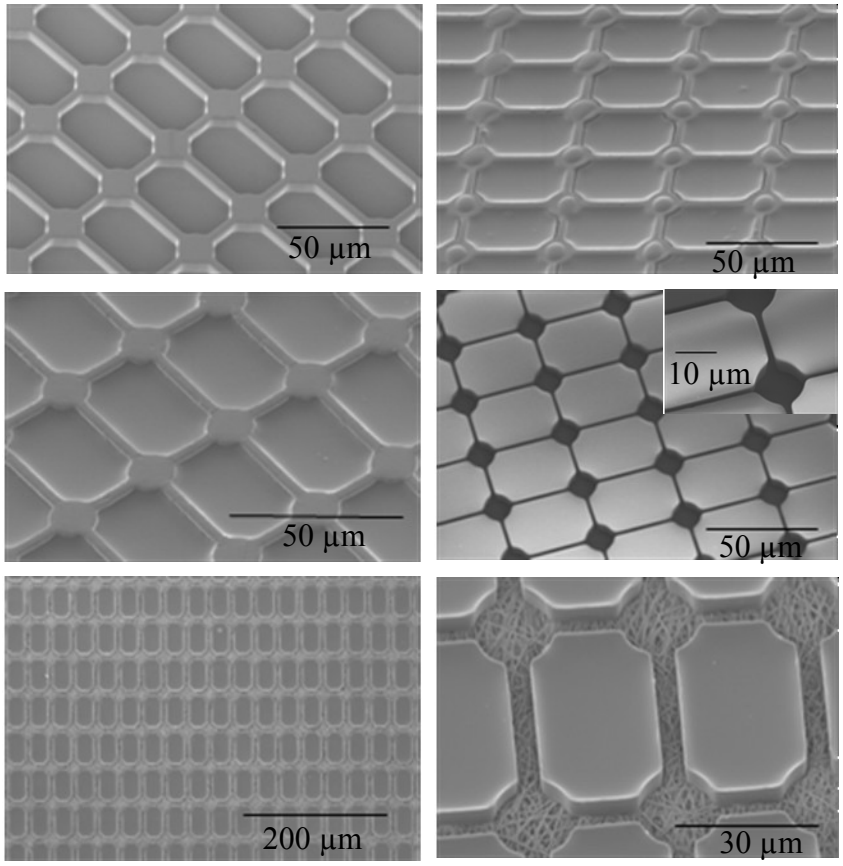

Figure 3.2 (A) PDMS Mold (B)Polymer Dewetting (C) Polymer removed from raised features (D) PS features standing on peeled off PVA film (E - F) Fabricated CNN Microdevice

3.3.2 Characterization of Electrospun Random Nanofibers

Electrospun Gel/PCL random nanofibers had diameter of 441 ± 141 nm. Figure 3.3 shows the SEM micrographs of electrospun Random Gel/PCL nanofibers.

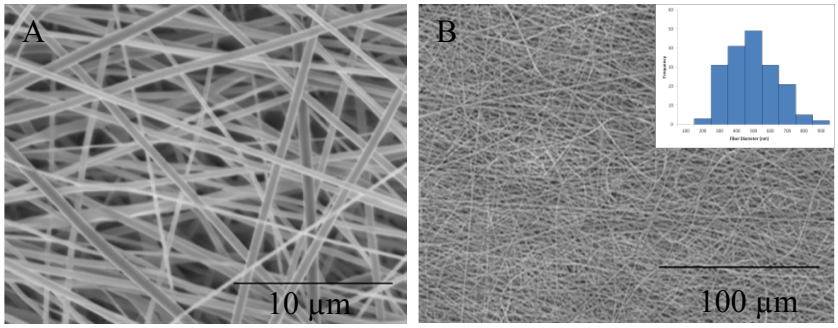

Figure 3.3 (A - B) Electrospun Random Gel/PCL Nanofibers

3.3.3 Patterning of PC12 Cells

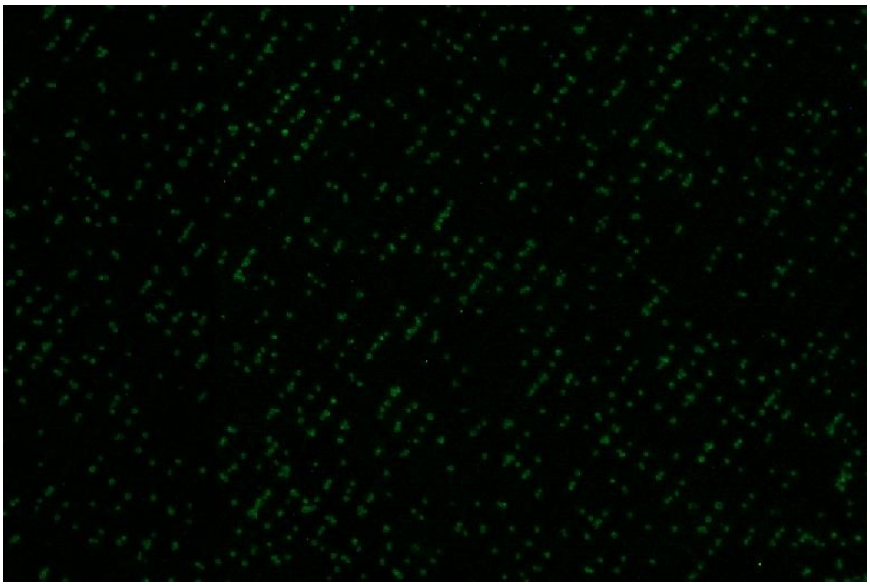

Figure 3.4 Cell Patterning on CNN Microdevice (green Alexafluor 488 phalloidin)

3.3.4 Adhesion of PC12 Cells

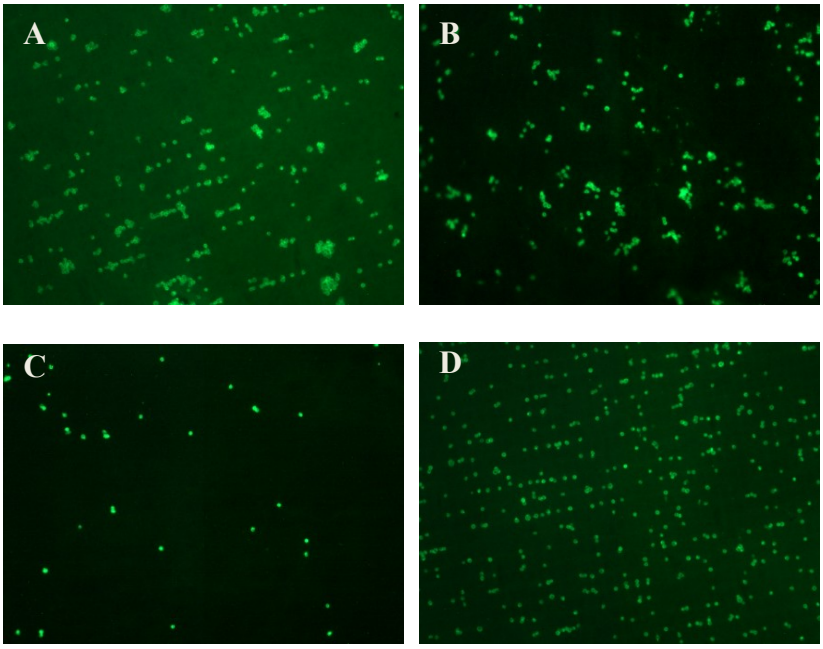

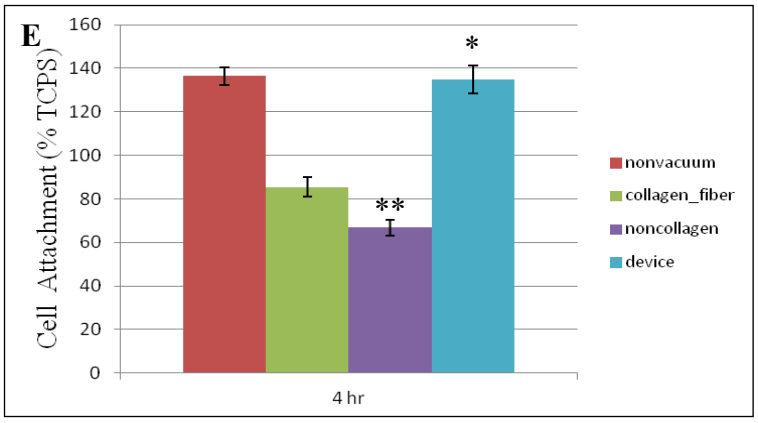

Figure 3.5 Representative images for attachment of PC12 Cells on: (A) nonvacuum; (B) collagen_fiber; (C) noncollagen; (D) device. (E) Cell Attachment (% TCPS) (* $p < 0.05$ relative to fiber controls, ** $p < 0.05$ relative to all other samples)

Fig. 3.5 (A-D) shows representative images of all of the samples following the adhesion assay. Adhesion results (Fig. 3.5 (E)) showed that device had significantly higher number of cell attachment compared to collagen_fiber, noncollagen and TCPS (* $p <$ 0.05). This suggests that the device is enhancing cell attachment and cell trapping within the CNN pattern. All collagen coated substrates had significantly higher number of cell attachment compared to noncollagen (** $p < 0.05$). Greater adhesion of PC12 cells on all substrates coated with collagen compared to noncollagen suggests that collagen is promoting cell attachment.

3.3.4 Viability of PC12 Cells

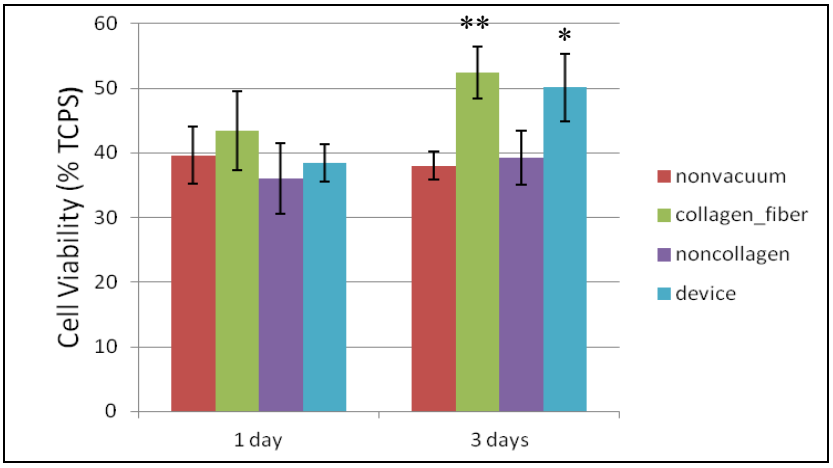

Figure 3.6 Viability of PC12 Cells on nonvacuum, collagen_fiber, noncollagen and device (* $p < 0.05$ compared to nonvacuum, ** $p < 0.05$ compared to noncollagen)

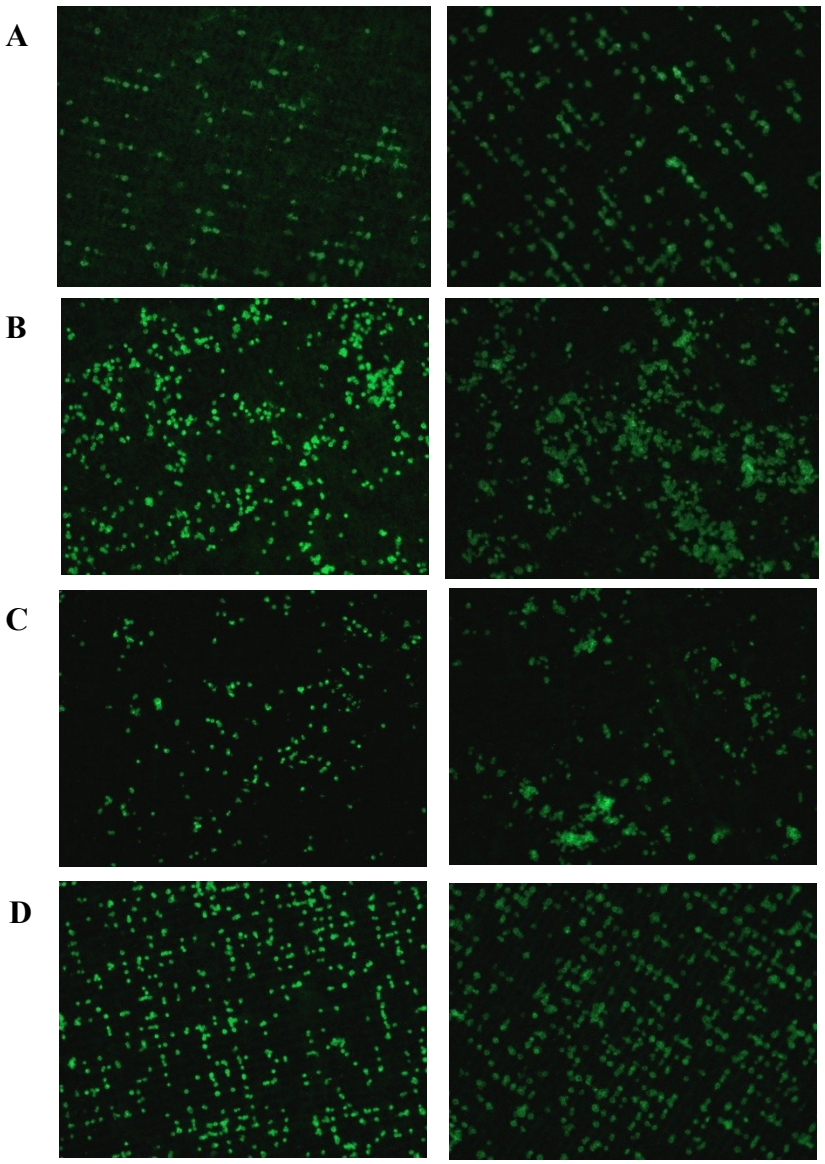

Figure 3.7 Representative images for viability of PC12 cells on: (A) nonvacuum; (B) collagen_fiber; (C) noncollagen; (D) device. (left, 1 day; right 3 days; green alexa fluor 488 phalloidin)

Fig. 3.7 (A-D) shows representative images of all of the samples following the viability assays. Viability assays (Figure 3.6) showed that the device had similar viability compared to collagen_fiber. This result suggests that during our process and fabrication there is no change to the collagen coating on the nanofibers or a significant change to the nanofiber morphology that could alter results. The device had significantly higher viability compared to nonvacuum samples (* $p < 0.05$) at day 3. Lower value of viability on nonvacuum samples suggests that without vacuum seeding cells had a lower probability of reaching to the nanofibers underneath the PS pattern. PC12 cells do not like untreated PS surface and have a very low attachment. Therefore seeding without vacuum results in a higher number of cluster formed during and after seeding. In addition, because of low attachment capability of cells to the PS, during medium change cells on the PS surface are washed away causing cell loss and remaining cells are pushed in the direction of cluster formation. Samples of collagen_fiber had significantly higher viability compared to noncollagen (** $p < 0.05$) at day 3. This result suggests that collagen increases cell attachment and viability. Collagen is the major component of ECM and is one of the ligand for the integrin receptors on the cells. Our results comply with previous work [107] that samples that are not coated with collagen had lower cell attachment and viability compared to all other samples coated with collagen.

3.3.5 Differentiation and Neurite Length

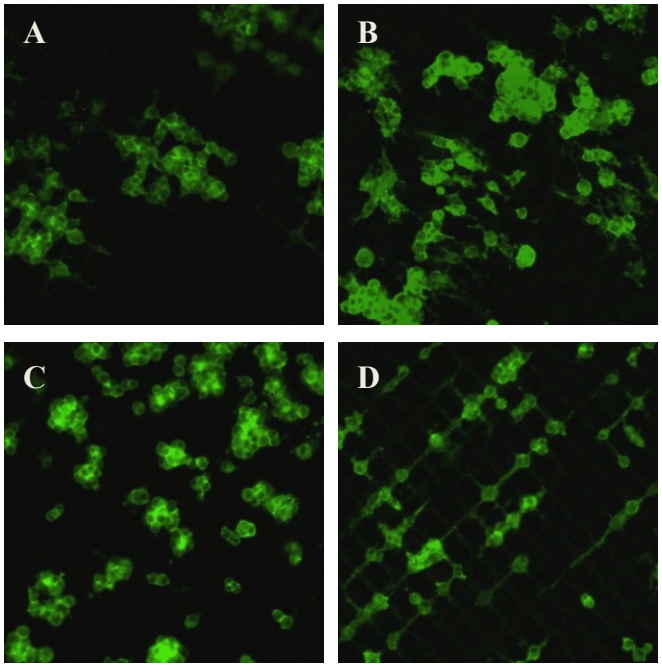

Figure 3.8 Differentiation of PC12 cells on: (A) nonvacuum (B) collagen_fiber (C) noncollagen (D) device

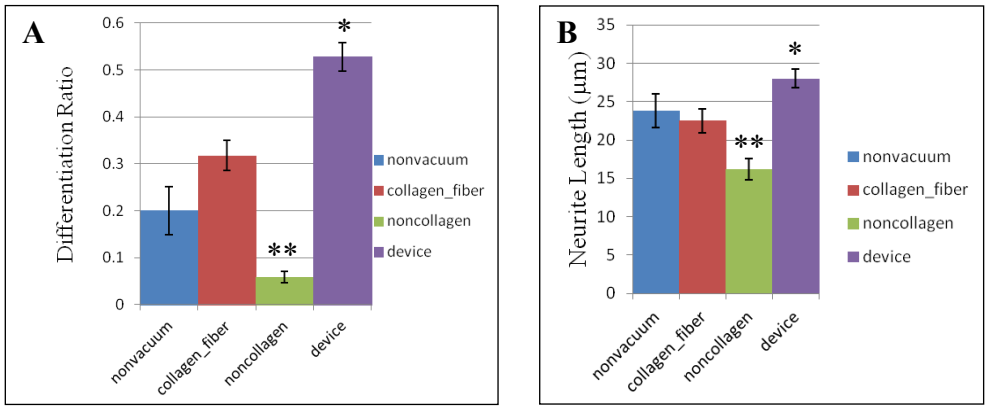

Figure 3.9 (A) Differentiation Ratio (* $p < 0.01$ compared to all controls, ** $p < 0.05$ compared to all other samples) and (B) Neurite Length (µm) (* $p < 0.05$ compared to all controls, ** $p < 0.05$ compared to all other samples)

Fig. 3.8 (A-D) shows representative images of all of the samples following the differentiation assays . The device had higher differentiation ratio (Fig. 3.9 (A)) and neurite length per differentiated cell (Fig. 3.9 (B)) compared to colllagen_fiber, nonvacuum and noncollagen. Significant difference were obtained for both differentiation ratio (* $p < 0.01$) and neurite length (* $p < 0.05$) when compared to all other controls. Lower ratio of differentiation on nonvacuum samples suggests that without vacuum seeding cells had a lower probability of reaching to the nanofibers underneath the PS pattern. PC12 cells do not like untreated PS surface and have a very low attachment. Some of the cells that were not in contact with the nanofibers were washed away during medium change. Hydrophobicity of untreated PS surface forces cells to form cluster around the cell which was located in the microwell. An increased cluster formation then reduces differentiation ratio. Lower differentiation ratio of collagen_fiber compared to the device suggests that not having a CNN pattern on the collagen_fiber samples did not provide physical separation of cells during initial seeding, leading to cluster formation at the beginning. As the time period increases, proliferation causes non-differentiated cell number to increase and at the end this leads to a reduced differentiation ratio. The device on the other hand, due to the CNN pattern can physically separate cells during initial seeding and reduce this cluster formation at the beginning. Considering the viability results, the device is indifferent in terms of proliferation after the initial cell seeding. Taken together, at the end of the prescribed time, device gets higher differentiation ratio compared to all other controls.

The device was able to pattern neuronal networks whereas all other controls could not. The CNN pattern allows physical separation of cells during seeding and permitting extension of neurites only within the grooves and thereby organizing the network formation and at the same time preventing cluster formation which facilitates differentiation of individual cells.

Lower ratio of differentiation on collagen_fiber compared to the device suggests that the proliferation of PC12 cells on collagen coated nanofibers is higher. This could be due to the clusters formed during initial seeding. The initial seeding density used for all experiments could be a relatively high density compared to previous works reported on differentiation of PC12 cells. Substrates other than the device are not suitable for differentiating PC12 cells at this density. Previous work have obtained similar differentiation ratio with the device but with a much lower seeding density. This seeding density allows us to pattern neuronal cells. The device not only allow patterning neuronal cells with a high density but allow differentiation of PC12 cells as well with a high density compared to previous work [104].

All substrates coated with collagen had higher differentiation ratio (** $p < 0.05$) and neurite length (** $p < 0.05$) compared to noncollagen substrate. Low differentiation ratio of noncollagen samples compared to all samples suggests that collagen promotes nerve regeneration [108].

A significantly lower differentiation ratio on the noncollagen samples suggests that even though the samples are continually supplied with NGF, the lack of collagen coating prevents the cross talk between tyrosine kinase receptor signaling and integrin

signaling in these samples. When the substrates were collagen coated, the cells in contact with the surface could differentiate, whereas cells on top of the clusters could not. This suggests that contacting collagen on the fiber surface activates the integrin signaling pathway, which then cross talks with the tyrosine kinase receptor pathway, leading to neurite differentiation [104, 116, 117].

3.4 Conclusions

In this chapter, we fabricated CNN devices and evaluated its performance with adhesion, viability and differentiation assays. The device demonstrated enhanced biocompatibility that it had increased adhesion compared to collagen_fiber, noncollagen and TCPS. It had also increased differentiation ratio and neurite length compared to all controls. In terms of proliferation, the device was indifferent compared to collagen_fiber.

CHAPTER 4: EFFECTS OF CELL CONFINEMENT AND NANOFIBER ORIENTATION ON NEURONAL NETWORK DIFFERENTIATION

4.1 Introduction

Peripheral nerve injury due to traumas may lead to sensorimotor defects because of not having a sophisticated repairing technique. Clinically, the injury is either coaptated from the transected part or if there is a large defect, an autograft is used. An autograft from the patient transplanted into the defective site can give functional recovery however this solution has drawbacks such that the donor site has limited availability and possible loss of function at the donor site. An alternative solution is the allograft which is a transplant from another human being or an animal. However, this technique causes immune problems at the host site. Therefore, artificial nerve guidance conduits (NGC) is a solution to this clinical problem that it can guide the axon and regenerate the defective nerve [63].

Examples for synthetic NGCs are microchannels, microfibers and hollow fiber membranes. These have advantages of increased availability, not needing a surgery for the donor site and better fixing of the axon at the suture site. NGCs have shown great promise *in vitro* but it is difficult to direct axon and regenerate nerve *in vivo*. In addition NGCs cannot respond to a nerve defect, which is above a critical length. NGCs cannot

selectively guide sensory or motor axons toward the end organs and due to their rigid structures there are issues of handling during the operation and implantation. Electrospun nanofibers due to their nanoscale feature size, fibrous morpghology mimicking ECM, being functionalized with or encapsulating bioactive molecules and anisotropic properties offer superior advantages over these techniques.

Electrospun nanofibers also has emerged as a tool to differentiate stem cells.

Xia et al. [67] have demonstrated that embryonic stem cells that are seeded onto aligned PCL nanofibers can differentiate into neural lineages. In addition, the neurite outgrowth was in the direction of aligned nanofibers. Results of O4 staining which is an antibody for oligodentrocyte specific glycolipid shows multipolar morphology on the nanofibers.

4.2 Materials and Methods

4.2.1 Materials

PCL (Mw = 65,000) , porcine gelatin type A and PS (Mw = 350,000) were obtained from Sigma-Aldrich Inc. Rat pheochromocytoma cell-line, PC12 was obtained from American Type Culture Collection (ATCC) and mouse 2.5S nerve growth factor (NGF) was obtained from Promega Corp.

4.2.2 CNN Device Fabrication

A negative photoresist SU8 2005 was spin coated onto silicon wafer with 3000 RPM. A grid pattern of recessed features (line width, 3 um; node diameter, 15 um, longer groove 30 um, shorter groove 15 um) on a chrome mask was transferred onto photoresist by ultraviolet (UV) photolithography. Polydimethylsiloxane (PDMS) was mixed with 10:1 curing agent and poured onto silicon master. After curing at room temperature for 2 days, negative replica was peeled off.

CNN microdevices are fabricated through a modified version of double stamp micromolding technique. 11 wt % polystyrene (PS) dissolved in anisole was drop cast and spin coated at 3500 RPM onto the PDMS mold (Figure 4.1 (a-b)). Polymer dewetted (Figure 4.1 (c)) and excess polymer on the raised features was removed by pressing onto a glass slide at 100 ^{o}C (Figure 4.1 (d)). 8 wt% polyvinyl alcohol (PVA) dissolved in deionized (DI) water and applied to the mold (Figure 4.1 (e)). After 1 day at room temperature, water is evaporated from the PVA solution and the mold is annealed for 1 min at 150 ^{o}C. The mold is cooled down for 15 minutes and PVA film is peeled off (Figure 4.1 (f)) from the PDMS mold and thereby also peeling off the PS features from the mold. Next, PS features standing on the PVA film is stamped onto the collagen coated aligned nanofibers at ~50 ^{o}C with applying ~100 psi (Figure 4.1 (g)) by aligning the aligned direction of nanofibers with the longer groove or shorter groove of the grid pattern under optical microscopy . Collagen coated stamped aligned nanofibers are then soaked in DI water for 1 hr for PVA film to dissolve and leaving PS features transferred onto the collagen coated aligned nanofiber mat (Figure 4.1 (h)).

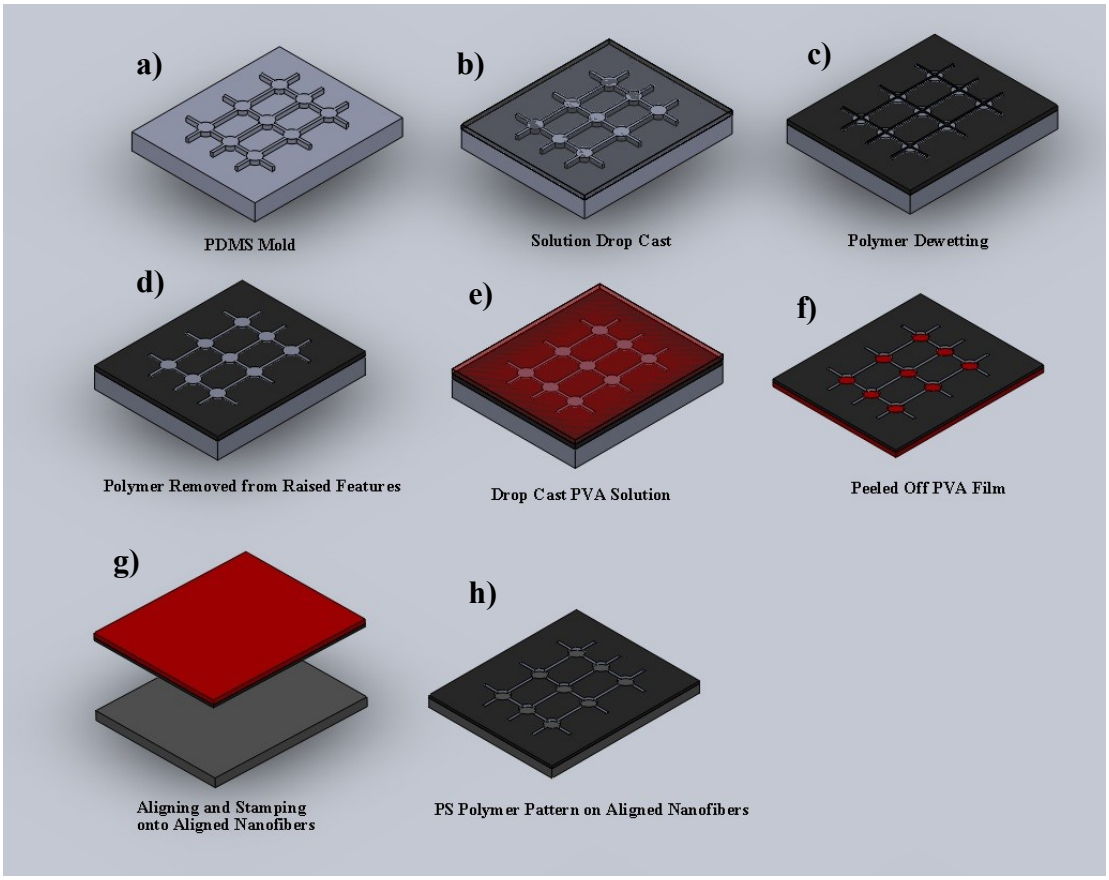

Figure 4.1 Fabrication of the CNN Microdevice on Electrospun Aligned nanofibers

4.2.3 Fabrication of Electrospun Aligned and Random Nanofibers

Gel 6.7 wt % in 1,1,1,3,3,3-hexafluoro-2-propanol (HFIP) and PCL 5 wt % in HFIP solutions are prepared separately by stirring them overnight at room temperature. The Gel and PCL solutions are then blended with 20:80 weight ratio and stirred for 1 hr. In a chemical hood, the blended solution is placed into a 20 cc syringe and was electrospun onto a rotating mandrel collector covered with aluminum sheet, using high-voltage DC power supply. Distance to the collector was 20 cm and the collector was set to -6kV,

controlled by a motor and was rotating at 500 rpm for aligned and 300 rpm for random nanofibers at all times. Electrospun aligned and random nanofibers are produced in 2 sets of electrospinning parameters. First, the solution was fed with 15 ml/hr for ½ hr through 20 G blunt tip and the applied potential was set to 20kV. Second, the solution was fed with 1 ml/hr for 3/2 hr through 25 G blunt tip and the applied potential was set to 13kV. Aligned and random nanofiber scaffolds were then kept in vacuum oven overnight for the remaining solvent to evaporate.

4.2.4 Collagen Coating onto Electrospun Aligned and Random Nanofibers

Electrospun aligned and random nanofibers are treated with oxygen (O_2) plasma for 1 min in an inductively coupled plasma cleaner. The radio frequency (RF) power was set to 50 W and the flow rate was set to 30 sccm. O_2 plasma treated aligned and random nanofibers are then immersed into the collagen solution of 300 µg/ml in 0.02 N Acetic Acid (AA) overnight at 4 ^{o}C. Scaffolds are then first washed with Phosphate Buffered Saline (PBS) for 5 min and secondly, 5 min with DI water and finally are air dried.

4.2.5 Characterization of the Electrospun Aligned and Random Nanofibers and the Fabricated CNN Device

Electrospun aligned and random nanofibers and the fabricated CNN microdevice are coated with a thin Au-Pd layer using a sputter coater and then characterized with scanning electron microscopy (SEM) operating at 5 kV. The electrospun aligned and random nanofiber diameter is measured based on the SEM micrographs (n=5) using an

image analysis software (imageJ; National Institute of Health, Bethesda, MD). Gelatin content of the scaffolds was confirmed previously[26].

4.2.6 Vacuum Assisted Cell Seeding

For all experiments, all of the electrospun aligned and random nanofiber based samples are cut into 23x23 mm^2 and are immersed in 70 % Ethanol (v/v) for 1 hr, washed with PBS 3 times and air dried. Sterilized 10 mm diameter PDMS rings applied with high vacuum grease are placed on all samples. Vacuum assisted cell seeding with a vacuum pressure of 5-10 in Hg is used on the samples needing it.

4.2.7 Sample Types

Five types of sample are used:

1) Fabricated CNN Microdevice seeded with vacuum pressure and aligned in the longer groove (long)

2) Fabricated CNN Microdevice seeded with vacuum pressure and aligned in the shorter groove (short)

3) Collagen coated aligned Get/ PCL electrospun nanofibers mat with cells seeded with vacuum pressure (aligned)

4) Collagen coated random Gel/PCL electrospun nanofiber mat with cells seeded with vacuum pressure (random)

5) Collagen coated tissue culture polystyrene (TCPS) as a control.

10 mm diameter PDMS rings are sealed onto tcps wells of a 12 well plate. Collagen solution is applied overnight onto tcps at room temperature and washed 3 times with sterile PBS.

4.2.8 In Vitro Cell Culture

A neuronal cell line, PC-12 cells were cultured in 75 cm^2 tissue culture flasks at 37 ^oC and 5% CO_2. Their media was RPMI 1640 (ATCC) with supplements of 10 % Horse Serum, 5% Fetal Bovine Serum, 1% Penicillin/Streptomycin (Complete Medium). The passage numbers of PC12 cells were kept at 10-20 for all experiments. Cells are seeded onto all samples with a density of 73800 cells/cm^2 for all experiments and 0.2 % Amphotericin B is added to all experimental cultures.

4.2.9 Cell Viability Assay

Cell Viability of the samples in 12-well plate were analyzed by Alamar Blue assay after 1 and 3 days of culture with the complete medium changing every other day. After 1 day, PDMS rings are removed from the culture. At the end of the prescribed time samples are washed with PBS and incubated for 3 hr in dark in fresh complete medium which is mixed with Alamar Blue assay reagent 10:1. Aliquots were pipetted into wells of a 96-well plate to be analyzed with a spectrophotometric plate reader. The fluorescence at 590 nm for each well was recorded. Values are normalized to 1 day TCPS control.

4.2.10 Immunoctyochemistry and Neurite Length

For differentiation studies samples are cultured in 12-well plate and after the first 6 hr, samples are washed with PBS and they were put back into fresh complete medium containing 100 ng/ml Nerve Growth Factor (NGF). After the first 12 hr, the culture medium was changed to RPMI 1640 Medium, 1% Horse Serum, 1% Penicillin/Streptomycin and 100 ng/ml NGF (Differentiation Medium). Differentiation medium was changed every other day.

After 4 days PDMS rings are removed from the culture, samples are washed with PBS and fixed with 4% paraformaldehyde for 15 min at room temperature followed by permeation with 0.3% Triton X-100 in PBS. Samples are washed 3 times with PBS for 5 min each and immersed in 5% Bovine Serum Albumin (BSA) in PBS for 1hr to block non-specific labeling. Samples are stained with anti-beta-tubulin monoclonal antibodies (1:500, Millipore) overnight at 4 ^{o}C. Samples are washed 3 times with PBS 5 min each and incubated in alexa fluor 546 conjugated donkey anti-mouse secondary antibodies (1:50) at 37 ^{o}C for 1hr in dark. Samples are washed 3 times with PBS for 5 min each and actin filaments were stained with Alexa Fluor 488 labeled phalloidin (Invitrogen) for 30 min at room temperature followed by 3 times PBS wash 5 min each and counterstained with 4',6-diamidino-2-phenylindole dilactate (Dapi, Invitrogen) for 5 min. Samples are washed 3 times with PBS for 5 min each and viewed by Nikon Ti Microscope. 10 Random fields per sample at 40x lens were collected. The number of differentiated cells were determined by having at least one neurite equal to or greater than 5 μm in length and were reported as a percentage of total number of cell nuclei in the field. Neurite

length was measured with imagej. If a neurite had branches, the branch length was calculated from the branching point.

4.2.11 Statistics

All data presented are expressed as mean ± standard deviation (SD). Results were subjected to unpaired student's *t*-test for statistical significance analysis ($p < 0.05$). Each parameter was conducted in triplicate (n=3) samples.

4.3 Results and Discussions

4.3.1 Fabricated CNN Microdevice

SEM micrographs of the device fabrication process and the final CNN microdevice on nanofibers platform are shown below (Figure 4.2) The fabricated CNN microdevices had ~5 um groove widths and ~18 um well diameters.

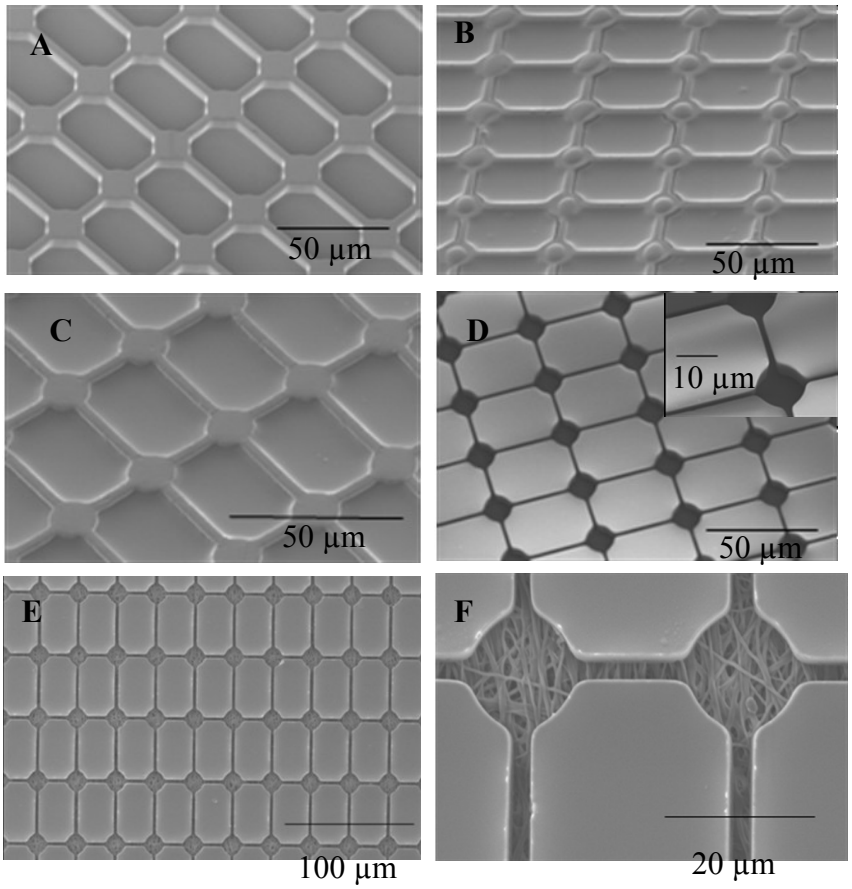

Figure 4.2 (A) PDMS Mold (B)Polymer Dewetting (C) Polymer removed from raised features (D) PS features standing on peeled off PVA film (E - F) Fabricated CNN Microdevice on Aligned Nanofibers

4.3.2 Characterization of Electrospun Aligned and Random Nanofibers

Electrospun Gel/PCL random nanofibers had diameter of 441 ± 141 nm. Electrospun Gel/PCL aligned nanofibers had diameter of 596 ± 194 nm. Figure 4.3 (A-D) shows the SEM micrographs of electrospun random and aligned Gel/PCL nanofibers.

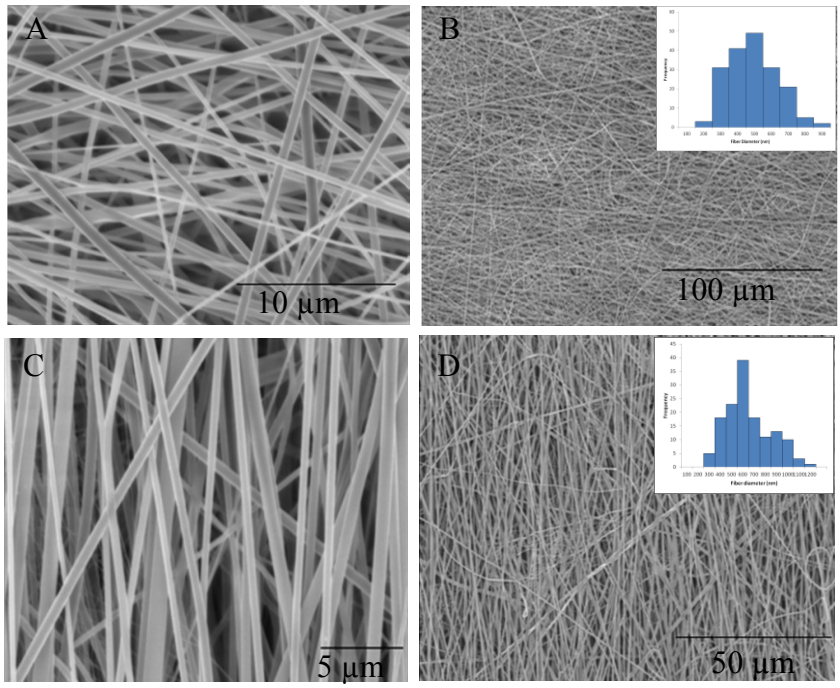

Figure 4.3 (A - B) Electrospun Random Gel/PCL Nanofibers (C - D) Electrospun Aligned Gel/PCL Nanofibers

4.3.3 Viability of PC12 Cells

Fig. 4.4 shows the data from the viability assays. As shown, at the Day 3 time point, both the long and short devices had significantly lower cell counts than the fiber controls (* $p<0.05$), but only slightly increased from their Day 1 values. Fig. 4.5 shows representative images of all of the samples following the viability assays. The long and the short devices had a slight increase in the number of cells at day 3, whereas on the control samples of aligned and random, the number of cells increased substantially at the end of the same prescribed time.

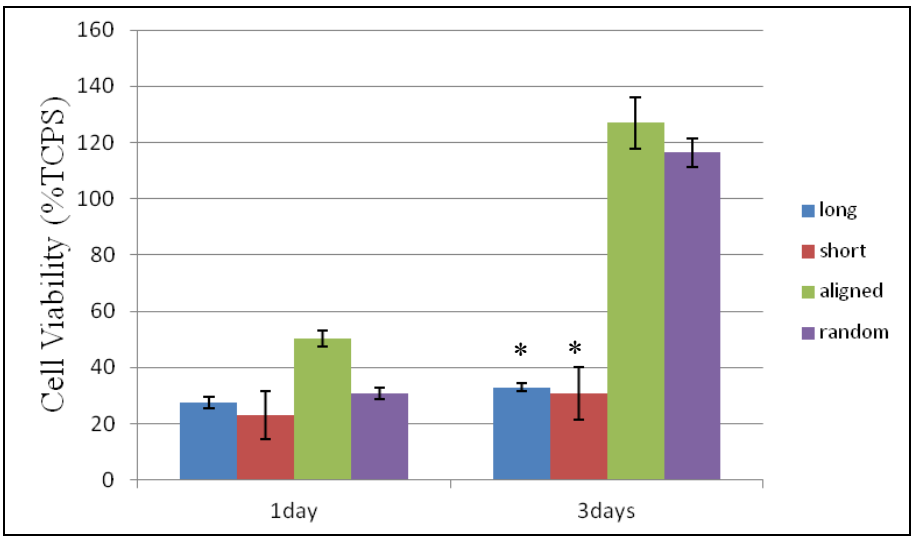

Figure 4.4 Viability of PC12 Cells on long, short, aligned and random (* $p < 0.05$ compared to fiber controls at day 3)

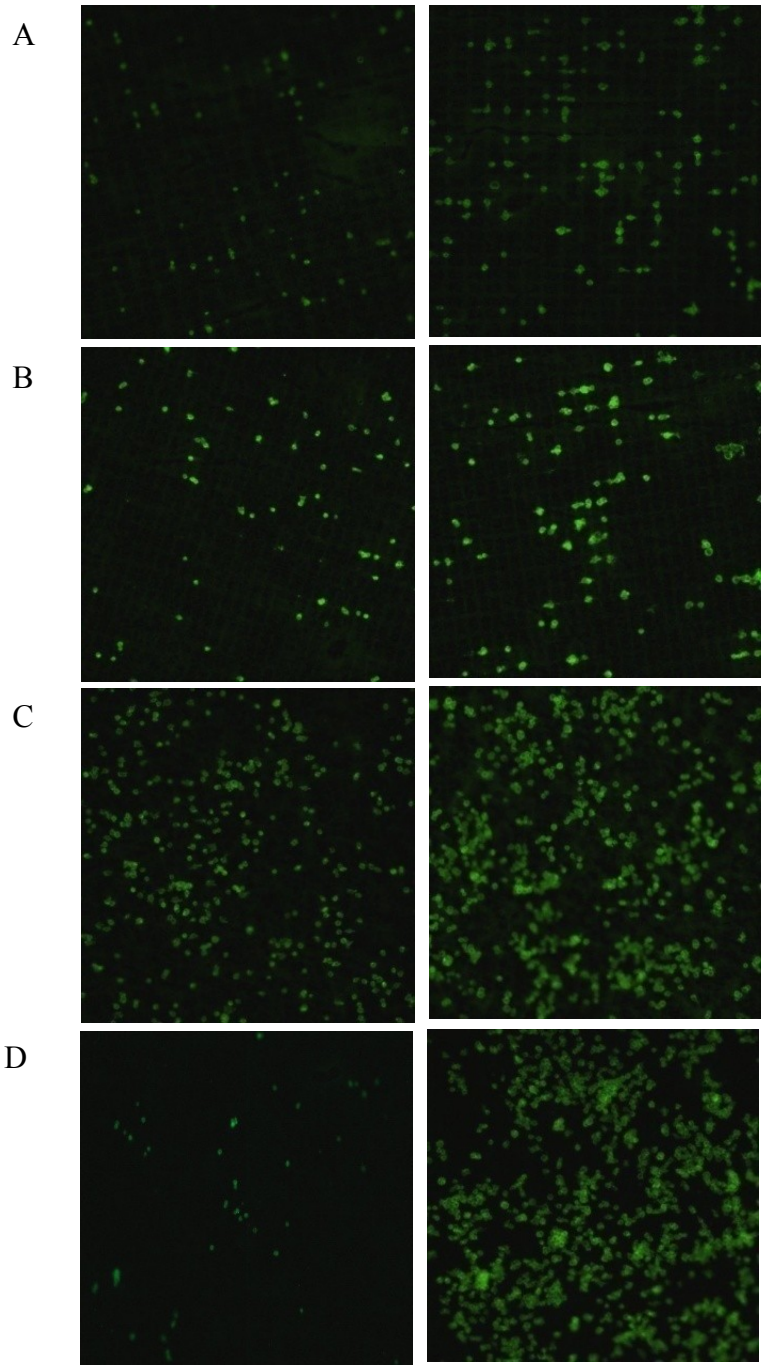

Figure 4.5 Representative images for viability of PC12 cells on: (A) long; (B) short; (C) aligned; (D) random. (left, 1 day; right 3 days; green alexa fluor 488 phalloidin)

4.3.4 Differentiation and Neurite Length

Fig. 4.6 shows representative images of all of the samples following the differentiation assays. The samples of long and short had significantly higher differentiation ratio (* $p < 0.05$, day 2; ** $p < 0.05$ day 4) compared to all other controls for all time periods, as shown in Fig. 4.7. Comparing between the long and the short, the long had significantly higher differentiation ratio for all time periods (*** $p< 0.05$ at day 2 and day 4) . The long and the short both had significantly higher average neurite length per differentiated cell compared to all other substrates for all time periods (* $p < 0.05$, day 2; ** $p < 0.05$ day 4), as shown in Fig. 4.8. There was significant difference in terms of viability between the long and the short (* $p<0.05$) and all other controls at day 3 as shown in Fig. 4.4. This viability result suggests that the long and the short were hindering proliferation which was desirable to promote differentiation. On control substrates however, proliferation and differentiation occurs at the same time after the differentiation medium is added. Control substrates do not have a CNN pattern and therefore they can not prevent cluster formation during initial cell seeding. As the time period increases cluster formation facilitates proliferation and at the end of the prescribed time, increased number of proliferated cells cause a reduced differentiation ratio.

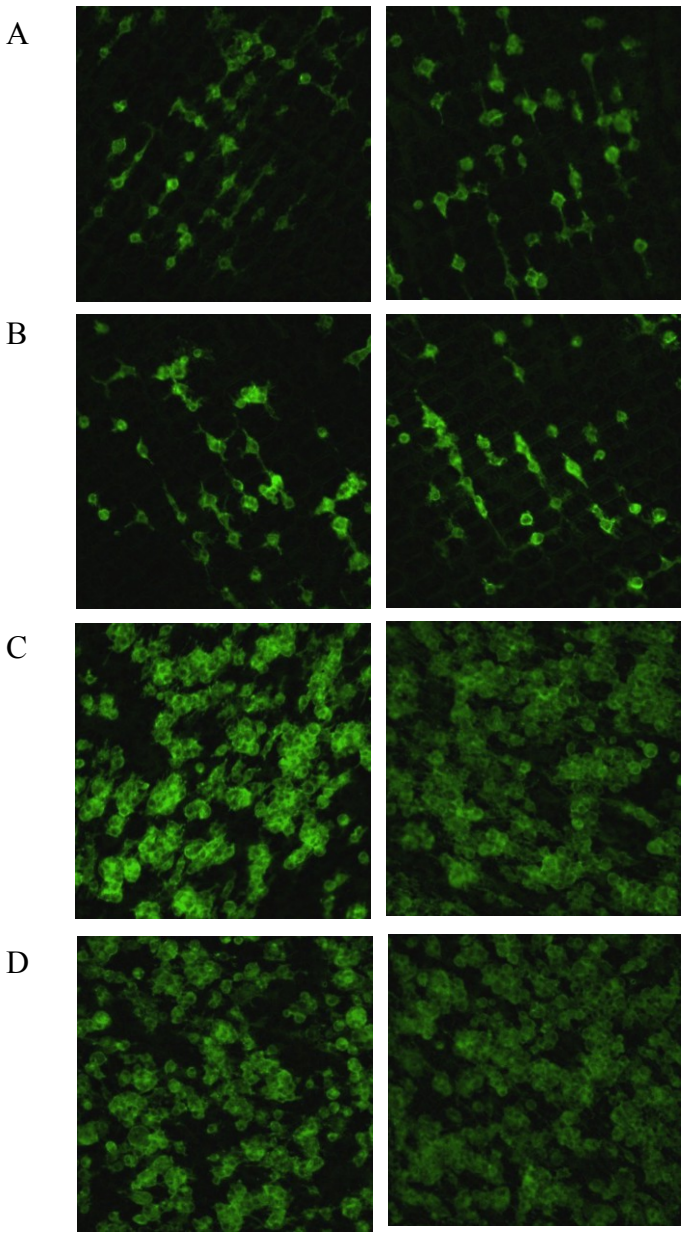

Figure 4.6 Representative images for Differentiation of PC12 cells on: (A) long; (B) short; (C) aligned; (D) random. (left, 2 days; right 4 days; green alexa fluor 488 phalloidin)

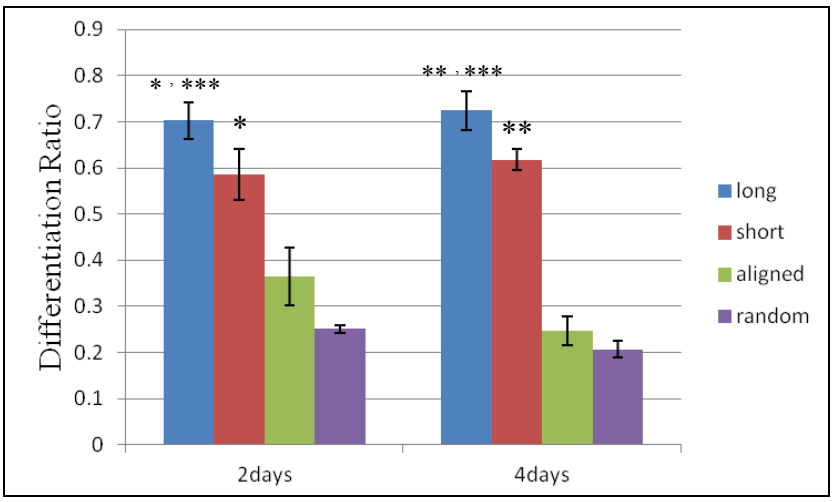

Figure 4.7 Differentiation Ratio (* p <0.05 compared to fiber controls at day 2, **p<0.05 compared to fiber controls at day 4, ***p<0.05 compared to short at days 2 and 4)

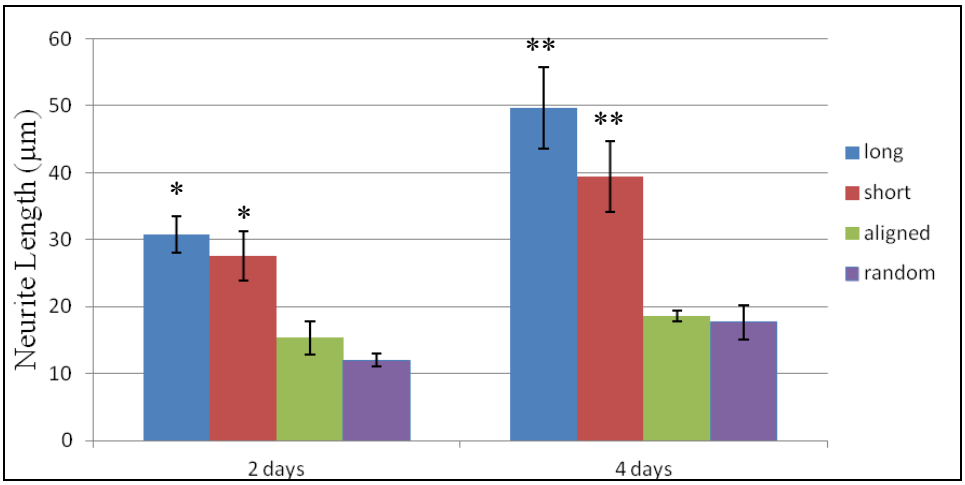

Figure 4.8 Average Neurite Length per Differentiated Cell (µm) (* p < 0.05 compared to fiber controls at day 2, ** p < 0.05 compared to fiber controls at day 4)

Increased neurite length on all substrates suggests that with increasing time, continued supplement of the growth factor increases neurite elongation. Higher

differentiation ratio and neurite length of the long compared to the short suggests that a longer groove promotes nerve differentiation and regeneration more than a shorter groove. A longer groove keeps a longer separation distance between neighboring cells and increases probability of nerve differentiation. In addition, the longer groove causes an increased effect of nanofiber alignment on PC12 cell differentiation.

Comparing these results to those from Chapter 3, the long and the short samples had higher differentiation ratio compared to the device on random nanofibers. This suggests two means of increasing the differentiation: decreasing the proliferation of cells prior to addition of the differentiation medium, and the contact guidance on aligned nanofibers which enhances nerve differentiation and nerve regeneration. Effects of anisotropy and togographical guidance to stem cell differentiation is reported in the literature as well. Wise et al. [112] reported that when human mesenchymal stem cells (hMSCs) were seeded onto electropun PCL nanofibers, differentiation into chondrogenic lineage was increased compared to PCL films. Kim et al. [113] seeed hMSCs onto nanografted PDMS structure and reported that differentiation into neuronal lineage was increased compared to non-patterned substrate.

Our results showed the long and the short are suitable for patterning neuronal networks and increase the probability of differentiation compared to controls.
In the collagen coated samples, the cells in contact with the surface could differentiate, whereas cells on top of the clusters could not. This suggests that cells in contact with the collagen on the nanofiber surface activated the integrin signaling pathway, which then

cross talked with the tyrosine kinase receptor, leading to neurite differentiation [104, 116, 117].

4.4 Conclusions

In this chapter, we fabricated CNN devices on aligned electrospun Gel/PCL nanofibers. Cell viability assays showed that the proliferation on the long and the short compared to controls were lower, indicating that the long and the short were more conducive to differentiate neuronal cells than controls. Differentiation assay showed that the long and the short enhanced differentiation and hindered proliferation due to the contact guidance on aligned nanofibers.

CHAPTER 5: CONCLUSIONS AND FUTURE WORK

Neuronal networks are groups of interconnected cells that can be a tissue slice, a population of cells *in vivo*, or a cultured group of cells *in vitro*. Neuronal networks are found in the Central Nervous System (CNS) or the Peripheral Nervous System (PNS) and can function in many different ways. They can be functioning unit in the sympathetic nervous system, a sensory circuit in spinal column, or a high level processing unit in a cerebral cortex. If neuronal networks lose their ability to perform their function, it ultimately leads to a neurological disorder in the body. In order to better diagnose and develop therapeutics for neurological disorders, it is important to better understand the underlying mechanisms of neurological disorders, and thus conducting research on neuronal networks becomes crucial for seeking cures for neurological disorders.

This dissertation explored the use of a confined neural network microdevice to better understand underlying mechanism of neurological disorders by simplifying, patterning and organizing neuronal networks. A patterned and simplified neuronal network can then provide more information about the disorder and can lead in the direction of finding a cure.

We fabricated the microdevices on ECM-like electrospun nanofibers to provide a more biomimetic substrate for our neuronal networks. We patterned neuronal-like PC12

cells and explored the biological response to our device on both random and aligned electrospun nanofibers by adhesion, viability, and differentiation assays.

In the first chapter, we discussed previous work on neuronal networks *in vitro* and *in vivo*, cell patterning, and applications of electrospun nanofibers in tissue engineering from the literature.

In the second chapter, we discussed the methodology to fabricate CNN devices. The steps of photolithography to pattern silicon wafer and soft lithography methods to mold PDMS were discussed. We used a double stamp micromolding technique, which is a modified version of microtransfer molding, to transfer PS grid pattern onto electrospun Gel/PCL nanofibers.

In the third chapter, we discussed the fabrication of our device on random electrospun Gel/PCL nanofibers. Using vacuum seeding, we obtained organized and patterned neuronal networks on electrospun random nanofibers. We evaluated the biological performance of our devices by adhesion, viability, and differentiation assays. We demonstrated that we could obtain a biocompatible device that patterns and organizes neuronal networks at higher densities and/or with higher differentiation rates than our controls. Our devices were indifferent in terms of proliferation after the physical separation during initial cell seeding. We also found that when the samples were not collagen coated, even though they were continually supplied with NGF, the cells had very low levels of differentiation. Due to a lack of collagen coating, it is possible that the cross talk between tyrosine kinase receptor signaling and integrin signaling did not occur on these samples. The presence of gelatin in the nanofibers may have provided enough

signaling for the portion of cells that did differentiate to signal the integrin signaling pathway. When the substrates were collagen coated, the cells in contact with the surface could differentiate whereas cells on top of the clusters could not. This suggests that contact with the collagen surface activates the integrin signaling pathway, which then cross talks with the tyrosine kinase receptor that leads to neurite differentiation [104, 116, 117].

In the fourth chapter, we fabricated our devices on aligned nanofibers to examine the effects of aligned fibers on the proliferation and differentiation of neurons for studying neural tissue engineering and nerve regeneration. We explored the effects of physical separation during initial cell seeding, nanofiber alignment and groove length on differentiation and neurite outgrowth. We demonstrated that a CNN on aligned nanofibers provides a platform that greatly enhances our ability to produce neural networks with highly differentiated neurons. We also demonstrated that a CNN device inhibits proliferation, and when the nanofiber is aligned with the longer groove, the CNN device has the highest differentiation ratio and causes the highest influence of nanofiber alignment on neuronal cell differentiation due to the contact guidance. We also found that when collagen coated samples in Chapter 4 could make contact with the fiber surface, they could differentiate, whereas cells on top of the clusters could not. This again suggests that contacting the collagen surface activates the integrin signaling pathway that then cross talks with the tyrosine kinase receptor and leads to neurite differentiation [104, 116, 117].

Overall, we found that there are three means of increasing differentiation: physical separation of cells during seeding (prevents cell cluster formation), contact guidance on aligned nanofibers (allows cell elongation and continuous neurite growth in a continuous direction), and collagen coating of the nanofibers (activates the integrin receptor signaling and cross talk with the kinase receptor pathway).

For future work, in terms of the device development, embedded electrodes into our devices will allow us to study plasticity and training of the neuronal networks we have obtained. In addition, by stacking these devices on top each other we can build a three dimensional device architecture that mimics more *in vivo* like behavior.

In terms of biological future work, the use of another cell line that is electrically active, or primary neurons, would tell us more about the information processing and exchange within the neuronal networks we have obtained. Electrophysiological recordings from an electrically active neuronal network on our devices would help us to better understand the underlying mechanism of neurological disorders and can lead in the correct direction to find a cure.

LIST OF REFERENCES

[1] T. Dua, M. G. Cumbrera, C. Mathers, S. Saxena, "Global burden of neurological disorders:estimates and projections", World Health Organization (2006) 27-41.

[2] J. Yamamoto, A. Ikeda, T. Satow, K. Takeshita, M. Takayama, M. Matsuhashi, R. Matsumoto, S. Ohara, N. Mikuni, J. Takahashi, S. Miyamoto, W. Taki, N. Hashimoto, J. C. Rothwell, H. Shibasaki, "Low-frequency electric cortical stimulation has an inhibitory effect on epileptic focus in mesial temporal lobe epilepsy" Epilepsia 43 (2002) 491-495.

[3] Y. Li, W. Zhou, X. Li, S. Zeng, M. Liu, Q. Luo, "Characterization of synchronized bursts in cultured hippocampal neuronal networks with learning training on microelectrode arrays" Biosensors and Bioelectronics 22 (2007) 2976–2982.

[4] F.L. Yap and Y. Zhang, "Protein and cell micropatterning and its integration with micro/nanoparticles assembly" Biosensors and Bioelectronics 22 (2007) 775–788.

[5] N. J. Ferrell, " Polymer microelectromechanical systems: fabrication and applications in biology and biological force measurements" Ph.D dissertation, The Ohio State University, 2008.

[6] M. J. Madou, "Fundamentals of microfabrication: the science of miniaturization" CRC Press, 2002.

[7] G. M.Whitesides, E. Ostuni, S. Takayama, X. Jiang, D. E. Ingber, "Soft lithography in biology and biochemistry" Annu. Rev. Biomed. Eng. 3 (2001) 335–373.

[8] Y. Xia and G. M. Whitesides, "Soft lithography" Annu. Rev. Mater. Sci. 28 (1998) 153–184.

[9] A. Kumar and G.M. Whitesides, "Features of gold having micrometer to centimeter dimensions can be formed through a combination of stamping with an elastomeric stamp and an alkanethiol ''ink'' followed by chemical etching" Applied Physics Letters 63 (1993) 2002-2004.

[10] A. Bernard, J. P. Renault, B. Michel, H. R. Bosshard, E. Delamarche, "Microcontact Printing of Proteins" Adv. Mater. 12 (2000) 1067-1070.

[11] H. Andersson and A. V. D. Berg, “Microfabrication and microfluidics for tissue engineering: state of the art and future opportunities” *Lab Chip* 4 (2004) 98-103.

[12] A. Papra, A. Bernard, D. Juncker, N. B. Larsen, B. Michel, E. Delamarche, “Microfluidic networks made of poly(dimethylsiloxane), Si, and Au coated with polyethylene glycol for patterning proteins onto surfaces” *Langmuir* 17 (2001) 4090–4095.

[13] A. M. Taylor, S. W. Rhee, C. H. Tu, D. H. Cribbs, C. W. Cotman, N. Li Jeon, “Microfluidic multicompartment device for neuroscience research” *Langmuir* 19 (2003) 1551–1556.

[14] P. Roacha, T. Parker, N. Gadegaard, M.R. Alexander, “ Surface strategies for control of neuronal cell adhesion: A review” *Surface Science Reports* 65 (2010) 145-173.

[15] C. F. Lu, A. Nadarajah, K. K. Chittur, “A comprehensive model of multiprotein adsorption on surfaces” *Journal of Colloid and Interface Science* 168 (1994) 152–161.

[16] F. Fang and I. Szleifer, “Kinetics and thermodynamics of protein adsorption: a generalized molecular theoretical approach” *Biophysical Journal* 80 (2001) 2568–2589.

[17] L.C. Xu, C. A. Siedlecki, “Effects of surface wettability and contact time on protein adhesion to biomaterial surfaces” *Biomaterials* 28 (2007) 3273–3283.

[18] H. Nygren, “Initial reactions of whole blood with hydrophilic and hydrophobic titanium surfaces” *Colloids and Surfaces B: Biointerfaces* 6 (1996) 329–333.

[19] J. J. A. Barry, D. Howard, K. M. Shakesheff, S. M. Howdle, M. R. Alexander, “Using a Core–Sheath Distribution of Surface Chemistry through 3D Tissue Engineering Scaffolds to Control Cell Ingress” *Advanced Materials* 18 (2006) 1406–1410.

[20] K. L. Prime and G. M. Whitesides, “Self-Assembled Organic Monolayers: Model Systems for Studying Adsorption of Proteins at Surfaces” *Science* 252 (1991) 1164–1167.

[21] E. T. Stoeckli, T. B. Kuhn, C. O. Duc, M. A. Ruegg, P. Sonderegger, “The axonally secreted protein axonin-1 is a potent substratum for neurite growth” *The journal of cell biology* 112 (1991) 449-455.

[22] H. Sorribas, C. Padeste, L. Tiefenauer, “Photolithographic generation of protein micropatterns for neuron culture applications” *Biomaterials* 23 (2002) 893–900.

[23] A. Offenhäusser, S. Böcker-Meffert, T. Decker, R. Helpenstein, P. Gasteier, J. Groll, M. Moller, A. Reska, S. Schäfer, P. Schultea, A. Vogt-Eisele, "Microcontact printing of proteins for neuronal cell guidance" *Soft Matter* 3 (2007) 290–298.

[24] M. Scholla, C. Sprösslerb, M. Denyerc, M. Krauseb, K. Nakajimac, A. Maelickea, W. Knollb, A. Offenhäusserb, "Ordered networks of rat hippocampal neurons attached to silicon oxide surfaces" *Journal of Neuroscience Methods* 104 (2000) 65–75.

[25] D. J. Fabrizius-Homan and S. L. Cooper, "Competitive adsorption of vitronection with albumin, fibrinogen, and fibronectin on polymeric biomaterials" *Journal of Biomedical Materials Research* 25 (1991) 953–971.

[26] L. Bużańska, A. Ruiz, M. Zychowicz, H. Rauscher, L. Ceriotti, F. Rossi, P. Colpo, K. Domańska-Janik, S. Coecke, "Patterned growth and differentiation of human cord blood-derived neural stem cells on bio-functionalized surfaces" *Acta Neurobiol* 69 (2009) 24-36.

[27] S. Xing, W. Liu, Z. Huang, L. Chen, K. Sun, D. Han, W. Zhang, X. Jiang, "Development of neurons on micropatterns reveals that growth cone responds to a sharp change of concentration of laminin" *Electrophoresis* 31 (2010) 3144–3151.

[28] A. Ruiz, L. Ceriotti, L. Buzanska, M. Hasiwa, F. Bretagnol, G. Ceccone, D. Gilliland, H. Rauscher, S. Coecke, P. Colpo, F. Rossi, "Controlled micropatterning of biomolecules for cell culturing" *Microelectronic Engineering* 84 (2007) 1733–1736.

[29] C. F. Amstein and P. A. Hartman, "Adaptation of plastic surfaces for tissue culture by glow discharge" *J. Clin. Microbiol.* 2 (1975) 46-54.

[30] A. Bruil, L. M. Brenneisen, J. G. A. Terlingen, T. Beugeling, W. G. Aken van, J. Feijen, "In vitro leukocyte adhesion to modified polyurethane surfaces. II. Effect of wettability" *Journal of Colloid and Interface Science* 165 (1994) 72-81.

[31] H. Hwang, G. Kang, J. H. Yeon, Y. Nam, J. K. Park, "Direct rapid prototyping of PDMS from a photomask film for micropatterning of biomolecules and cells" *Lab Chip* 9 (2009) 167-170.

[32] A. Rajnicek, S. Britland, C. McCaig, "Contact guidance of CNS neurites on grooved quartz: influence of groove dimensions, neuronal age and cell type" *Journal of Cell Science* 110 (1997) 2905-2913.

[33] J. Y. Lim, H. J. Donahue, "Cell sensing and response to micro- and nanostructured surfaces produced by chemical and topographic patterning" *Tissue Engineering* 13 (2007) 1879-1891.

[34] B. Wojciak-Stothard, A. Curtis, W. Monaghan, K. MacDonald, C. Wilkinson, "Guidance and activation of murine macrophages by nanometric scale topography" *Exp. Cell Res.* 223 (1996) 426-435.

[35] X. F. Walboomers, W. Monaghan, A. S. Curtis, J. A. Jansen, "Attachment of fibroblasts on smooth and microgrooved polystyrene" *J. Biomed. Mater. Res*. 46 (1999) 212-220.

[36] P. Clark, P. Connolly, A. S. Curtis, J. A. Dow, C. D. Wilkinson, "Topographical control of cell behaviour. I. Simple step cues" *Development* 99 (1987) 439-448.

[37] A. I. Teixeira, G. A. Abrams, P. J. Bertics, C. J. Murphy, P. F. Nealey, "Epithelial contact guidance on well-defined micro- and nanostructured substrates" *J. Cell Sci*. 116 (2003) 1881-1892.

[38] N. M. Dowell-Mesfin, M. A. Abdul-Karim, A. M. P. Turner, S. Schanz, H. G. Craighead, B. Roysam, J. N. Turner, W. Shain, "Topographically modified surfaces affect orientation and growth of hippocampal neurons" *J. Neural Eng*. 1 (2004) 78–90.

[39] D. Y. Fozdar, J. Y. Lee, C. E. Schmidt, S. Chen, "Selective axonal growth of embryonic hippocampal neurons according to topographic features of various sizes and shapes" *Int J Nanomedicine* 6 (2011) 45–57.

[40] A. M. Green, J. A. Jansen, J. P. van der Waerden, A. F. von Recum, "Fibroblast response to microtextured silicone surfaces: texture orientation into or out of the surface" *J. Biomed. Mater. Res*. 28 (1994) 647-653.

[41] J. A. Schmidt, A. F. von Recum, "Macrophage response to microtextured silicone" *Biomaterials* 13 (1992) 1059-1069.

[42] J. Zhanga, S. Venkataramania, H. Xua, Y. K. Songb, H. K. Songb, G. Tayhas, R. Palmoreb, J. Fallonc, A. V. Nurmikkoa, "Combined topographical and chemical micropatterns for templating neuronal networks" *Biomaterials* 27 (2006) 5734–5739.

[43] C. Miller, S. Jeftinija, S. Mallapragada, "Synergistic effects of physical and chemical guidance cues on neurite alignment and outgrowth on biodegradable polymer substrates" *Tissue Engineering* 8 (2002) 367-378.

[44] T. Subbiah, G. S. Bhat, R. W. Tock, S. Parameswaran, S. S. Ramkumar, "Electrospinning of nanofibers" *Journal of Applied Polymer Science* 96 (2005) 557–569.

[45] T. J. Sill, H. A. von Recum, "Electrospinning: Applications in drug delivery and tissue engineering" *Biomaterials* 29 (2008) 1989-2006.

[46] J. Xie, M. R. MacEwan, A. G. Schwartz, Y. Xia, "Electrospun nanofibers for neural tissue engineering" *Nanoscale* 2 (2010) 35–44.

[47] Q. P. PHAM, U. SHARMA, A. G. MIKOS, "Electrospinning of polymeric nanofibers for tissue engineering applications: A Review" *Tissue Engineering* 12 (2006) 1197-1211.

[48] J. M. Deitzel, J. Kleinmeyer, D. Harris, N. C. B. Tan, "The effect of processing variables on the morphology of electrospun nanofibers and textiles" *Polymer* 42 (2001) 261-272.

[49] G. Taylor, "Electrically driven jets" *Proc Natl Acad Sci London* 313 (1969) 453-475.

[50] S. Megelski, J. S. Stephens, D. B. Chase, J. F. Rabolt, "Micro and nanostructured surface morphology on electrospun polymer fibers" *Macromolecules* 35 (2002) 8456-866.

[51] J. Doshi and D. H. Reneker, "Electrospinning process and applications of electrospun fibers" *J Electrostatics* 35 (1995) 151-160.

[52] C. X. Zhang, X. Y. Yuan, L. L. Wu, Y. Han, J. Sheng, "Study on morphology of electrospun poly(vinyl alcohol) mats" *Eur Poly J* 41 (2005) 423-432.

[53] H. Jiang, D. Fang, B. S. Hsiao, B. Chu, W. Chen, "Optimization and characterization of dextran membranes prepared by electrospinning" *Biomacromolecules* 5 (2004) 326-333.

[54] K. Kim, M. Yua, X. Zonga, J. Chiuc, D. Fangb, Y. S. Seod, M. Hadjiargyrou, "Control of degradation rate and hydrophilicity in electrospun non-woven poly(D,L-lactide) nanofiber scaffolds for biomedical applications" *Biomaterials* 24 (2003) 4977-4985.

[55] E. R. Kenawya, J. M. Laymana, J. R. Watkinsa, G. L. Bowlinb, J. A. Matthewsb, D. G. Simpsonc, G. E. Wneka, "Electrospinning of poly(ethylene-co-vinyl alcohol) fibers" *Biomaterials* 24 (2003) 907-913.

[56] J. Stitzel, J. Liua, S. J. Leec, M. Komurac, J. Berrya, S. Sokerc, G. Limc, M. Van Dykec, R. Czerwb, J. J. Yooc, A. Atalac, "Controlled fabrication of a biological vascular substitute" *Biomaterials* 27 (2006) 1088-1094.

[57] C. Y. Xu, R. Inai, M. Kotaki, S. Ramakrishna, "Aligned biodegradable nanofibrous structure: a potential scaffold for blood vessel engineering" *Biomaterials* 25 (2004) 877-886.

[58] E. Schnell, K. Klinkhammer, S. Balzer, G. Brook, D. Klee, P. Dalton, "Et al. guidance of glial cell migration and axonal growth on electrospun nanofibers of poly-epsilon-caprolactone and a collagen/poly-epsilon-caprolactone blend" *Biomaterials* 28 (2007) 3012-3025.

[59] A. Cooper, N. Bhattarai1, M. Zhang, "Fabrication and cellular compatibility of aligned chitosan–PCL fibers for nerve tissue regeneration" *Carbohydrate Polymers* 85 (2011) 149–156.

[60] S. J. Eichhorn, W. W. Sampson, "Statistical geometry of pores and statistics of porous nanofibrous assemblies" *J R Soc Interface* 2 (2005) 309-318.

[61] W. J. Li, C. T. Laurencin, E. J. Caterson, R. S. Tuan, F. K. Ko, "Electrospun nanofibrous structure: a novel scaffold for tissue engineering" *J Biomed Mater Res* 60 (2002) 613-621.

[62] T. G. Kim, T. G. Park, "Biomimicking extracellular matrix: cell adhesive RGD peptide modified electrospun poly(D,L-lactic-co-glycolic acid) nanofiber mesh" *Tissue Eng* 2 (2006) 221-233.

[63] J. Xie, M. R. MacEwan, A. G. Schwartz, Y. Xia, "Electrospun nanofibers for neural tissue engineering" *Nanoscale* 2 (2010) 35–44.

[64] B. Dong, M. E. Smith, G. E. Wnek, "Encapsulation of Multiple Biological Compounds Within a Single Electrospun Fiber" *Small* 5 (2009) 1508–1512.

[65] V. Thomas, M. V. Jose, S. Chowdhury, J. F. Sullivan, D. R. Dean, Y. K. Vohra, "Mechano-morphological studies of aligned nanofibrous scaffolds of polycaprolactone fabricated by electrospinning" *J Biomater Sci Polym* Ed 17 (2006) 969-984.

[66] H. W. Ouyang, J. C. Goh, A. Thambyah, S. H. Teoh, E. H. Lee, "Knitted polylactide-co-glycolide scaffold loaded with bone marrow stromal cells in repair and regeneration of rabbit Achilles tendon" *Tissue Eng* 9 (2003) 431-439.

[67] J. Xie, S. M. Willerth, X. Li, M. R. Macewan, A. Rader, S. E. Sakiyama-Elbert, Y. Xia, "The differentiation of embryonic stem cells seeded on electrospun nanofibers into neural lineages" *Biomaterials* 30 (2009) 354–362.

[68] G. T. Christophersona, H. Songb, H. Q. Maoa, "The influence of fiber diameter of electrospun substrates on neural stem cell differentiation and proliferation" *Biomaterials* 30 (2009) 556–564.

[69] F. Yanga, R. Muruganb, S. Wangc, S. Ramakrishnaa, "Electrospinning of nano/micro scale poly(l-lactic acid) aligned fibers and their potential in neural tissue engineering" *Biomaterials* 26 (2005) 2603–2610.

[70] J. Xie, M. R. MacEwan, X. Li, S. E. Sakiyama-Elbert, Y. Xia, "Neurite Outgrowth on Nanofiber Scaffolds with Different Orders, Structures, and Surface Properties" *ACS Nano* 3 (2009) 1151–1159.

[71] S. Patel, K. Kurpinski, R. Quigley, H. Gao, B. S. Hsiao, M. M. Poo, S. Li, "Bioactive nanofibers: synergistic effects of nanotopography and chemical signaling on cell guidance" *Nano Lett.* 7 (2007) 2122–2128.

[72] M. P. Prabhakaran, J. Venugopal, C. K. Chan,S. Ramakrishna, "Surface modified electrospun nanofibrous scaffolds for nerve tissue engineering" *Nanotechnology* 19 (2008) 455102.

[73] E. Schnella, K. Klinkhammerb, S. Balzerc, G. Brookc, D. Kleeb, P. Daltonb, J. Meya, "Guidance of glial cell migration and axonal growth on electrospun nanofibers of poly-ε-caprolactone and a collagen/poly-ε-caprolactone blend" *Biomaterials* 28 (2007) 3012–3025.

[74] M. A. Alvarez-Perez, V. Guarino, V. Cirillo, L. Ambrosio, "Influence of gelatin cues in PCL electrospun membranes on nerve outgrowth" *Biomacromolecules* 11 (2010) 2238–2246.

[75] H.S. Koh, T. Yong, C. K. Chan, S. Ramakrishna, "Enhancement of neurite outgrowth using nano-structured scaffolds coupled with laminin" *Biomaterials* 29 (2008) 3574–3582.

[76] T. B. Bini, S. Gao, T. C. Tan, S. Wang, A. Lim, L. B. Hai, S. Ramakrishna, "Electrospun poly(L-lactide-co-glycolide) biodegradable polymer nanofibre tubes for peripheral nerve regeneration" *Nanotechnology* 15 (2004) 1459–1464.

[77] S. Y. Chew, R. Mi, A. Hoke, K. W. Leong, "Aligned Protein–Polymer Composite Fibers Enhance Nerve Regeneration: A Potential Tissue-Engineering Platform" *Advanced Functional Materials* 17 (2007) 1288–1296.

[78] L. Yao, N. O'Brien, A. Windebank, A. Pandit, "Orienting neurite growth in electrospun fibrous neural conduits" *Journal of Biomedical Materials Research Part B: Applied Biomaterials* 90B (2009) 483–491.

[79] X. M. Zhao, Y. Xia, G. M. Whitesides, "Fabrication of three-dimensional micro-structures: Microtransfer molding" *Advanced Materials* 8 (1996) 837–840.

[80] J. Guan, A. Chakrapani, D. J. Hansford, "Polymer microparticles fabricated by soft lithography" *Chem. Mater*. 17 (2005) 6227–6229.

[81] J. Guan, N. Ferrella, L. J. Leeb, D. J. Hansford, "Fabrication of polymeric microparticles for drug delivery by soft lithography" *Biomaterials* 27 (2006) 4034–4041.

[82] R. Günter, "Dewetting of thin polymer films" *Physical Review Letters* 68 (1992) 75-78.

[83] R. Xie, A. Karim, J. F. Douglas, C. C. Han, R. A. Weiss, "Spinodal dewetting of thin polymer films" *Physical Review Letters* 81 (1998) 1251-1254.

[84] N. Ferrell and D. Hansford, "Fabrication of micro- and nanoscale polymer structures by soft lithography and spin dewetting" *Macromol. Rapid Commun*. 28 (2007) 966–971.

[85] M. Scholl, C. Sprössler, M. Denyer, M. Krause, K. Nakajima, A. Maelicke, W. Knoll, A. Offenhäusser, "Ordered networks of rat hippocampal neurons attached to silicon oxide surfaces" *Journal of Neuroscience Methods* 104 2000 65-75.

[86] A. K. Vogt, G. J. Brewer, A. Offenhäusser, "Connectivity Patterns in Neuronal Networks of Experimentally Defined Geometry" *Tissue Engineering* 11 (2005) 1757-1767.

[87] J. C. Chang, G. J. Brewer, B. C. Wheeler, "Neuronal network structuring induces greater neuronal activity through enhanced astroglial development" *Journal of Neural Engineering* 3 (2006) 217-226.

[88] Peter Krsko, T. E. McCann, T. T. Thach, T. L. Laabs, H. M. Geller, M. R. Libera, "Length-scale mediated adhesion and directed growth of neural cells by surface-patterned poly(ethylene glycol) hydrogels" *Biomaterials* 30 (2009) 721-729.

[89] D. S. Finch, T. Oreskovic, K. Ramadurai, C. F. Herrmann, S. M. George, R. L. Mahajan, "Biocompatibility of atomic layer-deposidted alumina films" Journal of Biomedical Materials Research Part A 87A (2008) 100–106.

[90] C. G. Specht, O. A. Williams, R. B. Jackman, Ralf Schoepfer, "Ordered growth of neurons on diamond" *Biomaterials* 25 (2004) 4073–4078.

[91] J. C. Chang, G. J. Brewer, B. C. Wheeler, "Modulation of neuronal network activity by patterning" Biosensors and Bioelectronics 16 (2001) 527–533.

[92] N. Patel, R. Padera, G. H. W. Sanders, S. M. Cannizzaro, M. C. Davies, R. Langer, C. J. Roberts, S. J. B. Tendler, P. M. Williams, K. M. Shakesheff, "Spatially controlled

cell engineering on biodegradable polymer surfaces" *The FASEB Journal* 12 (1998) 1447-1454.

[93] D. Falconnet, A. Koenig, F. Assi, M. Textor, "A combined photolithographic and molecular-assembly approach to produce functional micropatterns for applications in the biosciences" *Advanced Functional Materials* 14 (2004) 749–756.

[94] W. C. Chang and D. W. Sretavan, "Novel High-Resolution Micropatterning for Neuron Culture Using Polylysine Adsorption on a Cell Repellant, Plasma-Polymerized Background" *Langmuir* 24 (2008) 13048–13057.

[95] A. Kumar, H. A. Biebuyck, G. M. Whitesides, "Patterning self-assembled monolayers: Applications in materials science" *Langmuir* 10 (1994) 1498–1511.

[96] J. Zhang, S. Venkataramani, H. Xu, Y. K. Song, H. K. Song, G. T. R. Palmore, J. Fallon, A. V. Nurmikko, "Combined topographical and chemical micropatterns for templating neuronal networks" *Biomaterials* 27 (2006) 5734–5739.

[97] N. M. Dowell-Mesfin, M. A. Abdul-Karim, A. M. P. Turner, S. Schanz, H. G. Craighead, B. Roysam, J. N. Turner, W. Shain, "Topographically modified surfaces affect orientation and growth of hippocampal neurons" *J. Neural Eng.* 1 (2004) 78–90.

[98] M. A. Alvarez-Perez, V. Guarino, V. Cirillo, L. Ambrosio, "Influence of gelatin cues in PCL electrospun membranes on nerve outgrowth" *Biomacromolecules* 11 (2010) 2238–2246.

[99] Y. Zhang, H. Ouyang, C. T. Lim, S. Ramakrishna, Z. M. Huang, "Electrospinning of gelatin fibers and gelatin/PCL composite fibrous scaffolds" *Journal of Biomedical Materials Research Part B: Applied Biomaterials* 72B (2005) 156–165.

[100] L. Ghasemi-Mobarakeh, M. P. Prabhakaran, M. Morshed, M. H. Nasr-Esfahani, S. Ramakrishna, "Electrospun poly(ε-caprolactone)/gelatin nanofibrous scaffolds for nerve tissue engineering" *Biomaterials* 29 (2008) 4532–4539.

[101] M. P. Prabhakaran, J. R. Venugopal, T. T. Chyan, L. B. Hai, C. K. Chan, A. Y. Lim, S. Ramakrishna, "Electrospun Biocomposite Nanofibrous Scaffolds for Neural Tissue Engineering" *Tissue Engineering Part A*. 14 (2008) 1787-1797.

[102] M. S. Kim, I. Jun, Y. M. Shin, W. Jang, S. I. Kim, H. Shin, "The development of genipin-crosslinked poly(caprolactone) (PCL)/gelatin nanofibers for tissue engineering applications" *Macromolecular Bioscience* 10 (201) 91–100.

[103] L. Ghasemi-Mobarakeh, M. P. Prabhakaran, M. Morshed, M. H. Nasr-Esfahani, S. Ramakrishna, "Electrospun poly(ε-caprolactone)/gelatin nanofibrous scaffolds for nerve tissue engineering" *Biomaterials* 29 (2008) 4532–4539.

[104] M. A. Alvarez-Perez, V. Guarino, V. Cirillo, L. Ambrosio, "Influence of gelatin cues in PCL electrospun membranes on nerve outgrowth" *Biomacromolecules* 11 (2010) 2238–2246.

[105] H.S. Koh, T. Yong, C. K. Chan, S. Ramakrishna, "Enhancement of neurite outgrowth using nano-structured scaffolds coupled with laminin" *Biomaterials* 29 (2008) 3574–3582.

[106] M. Cheng, W. Cao, Y. Gao, Y. Gong, N. Zhao, X. Zhang, "Studies on nerve cell affinity of biodegradable modified chitosan films" *J. Biomater. Sci. Polymer Edn.* 14 (2003) 1155– 1167.

[107] W. He, Z. W. Ma, T. Yong, W. E. Teo, S. Ramakrishna, "Fabrication of collagen-coated biodegradable polymer nanofiber mesh and its potential for endothelial cells growth" *Biomaterials* 26 (2005) 7606–7615.

[108] N. E. Zander, J. A. Orlicki, A. M. Rawlett, T. P. Beebe, "Surface-modified nanofibrous biomaterial bridge for the enhancement and control of neurite outgrowth" *Biointerphases* 5 (2010) 149-158.

[109] N. Ferrell and D. Hansford, "Fabrication of micro- and nanoscale polymer structures by soft lithography and spin dewetting" *Macromol. Rapid Commun*. 28 (2007) 966–971.

[110] Y. C. Lim, J. Johnson, Z. Fei, Y. Wu, D. F. Farson, J. J. Lannutti, H. W. Choi, L. J. Lee, "Micropatterning and characterization of electrospun poly(e-Caprolactone)/gelatin nanofiber tissue scaffolds by femtosecond laser ablation for tissue engineering applications" *Biotechnology and Bioengineering* 108 (2011) 116-126.

[111] N. Ferrell, D. Gallego-Perez, N. Higuita-Castro, R. T. Butler, R. K. Reen, K. J. Gooch, D. J. Hansford, "Vacuum-Assisted Cell Seeding in a Microwell Cell Culture System" *Anal. Chem*. 82 (2010) 2380–2386.

[112] J. Wise, A.L. Yarin, C. M. Megaridis, M. Cho, "Chondrogenic differentiation of human mesenchymal stem cells on oriented nanofibrous scaffolds: engineering the superficial zone of articular cartilage" *Tissue Engineering: Part A* 15 (2009) 913-921

[113] E. K.F. Yim, S. W. Pang, K. W. Leong, "Synthetic nanostructures inducing differentiation of human mesenchymal stem cells into neuronal lineage" *Experimental Cell Research* 313 (2007) 1820 – 1829

[114] D. H. J. van Weering and J. L. Bos, "Signal Transduction by the Receptor Tyrosine Kinase Ret" *Recent Results in Cancer Research* 154 (1998) 271-281

[115] D. Vaudry, P. J. S. Stork, P. Lazarovici, L. E. Eiden, "Signaling Pathways for PC12 Cell Differentiation: Making the Right Connections" *Science* 296 (2002) 1648-1649

[116] F. Q. Zhou and W. D. Snider, "Intracellular control of developmental and regenerative axon" *Phil. Trans. R. Soc. B* 361 (2006) 1575–159

[117] I. Ivankovic-Dikic, E. Grönroos, A. Blaukat, B. Barth, I. Dikic, "Pyk2 and FAK regulate neurite outgrowth induced by growth factors and integrins" *Nature Cell Biology* 2 (2000) 574-581

[118] J. L. Goldberg, "How does an axon grow?" *Genes and Development* 17 (2003) 941–958

[119]